Supporting Information

Design of an Amide *N*-glycoside Derivative of β-Glucogallin: A Stable, Potent, and Specific Inhibitor of Aldose Reductase

Linfeng Li,[†] Kun-Che Chang,[†, §] Yaming Zhou,[†] Biehuoy Shieh,[§] Jessica Ponder,[†] Adedoyin D. Abraham,[†] Hadi Ali,[†] Anson Snow,[§] J. Mark Petrash,[†,§] and Daniel V. LaBarbera[†,*]

[†]Department of Pharmaceutical Sciences, Skaggs School of Pharmacy and Pharmaceutical Science; and [§]Department of Ophthalmology, School of Medicine, University of Colorado Anschutz Medical Campus, Aurora, CO 80045, USA

*Address correspondese to DVL: daniel.labarbera@ucdenver.edu

Table of Contents

METHODS AND MATERIALS

All commercial chemicals were used as supplied unless otherwise indicated.All solvents were dried and distilled using standard protocols. All reactions were performed under an inert atmosphere of ultrapure nitrogen with oven-dried glassware unless otherwise noted. All organic extracts were dried over sodium sulfate. Thin layer chromatography (TLC) was performed using aluminum backed plates coated with 60Å Silica gel F_{254}. Plates were visualized using a UV lamp (λ_{max} = 254 nm) and/or by staining with phosphomolybdic acid solution (20 wt% in ethanol). Column chromatography was carried out using 230-400 mesh 60Å silica gel. Analysis of sample purity was performed on a Shimadzu Prominence HPLC system with a Phenomenex Kinetex C18 reversed phase column (5 µm, 100 Å, 250 × 4.6 mm). HPLC conditions: solvent A = H_2O, solvent B = MeCN; flow rate = 1.0 mL/min; compounds were eluted with a gradient of Water to MeCN over 30 min. All tested compounds have a purity ⩾95%.

Analytical Methods and Equipment: Proton (δ_H) and carbon (δ_C) nuclear magnetic resonances were recorded on a Varian INOVA 500 MHz spectrometer (500 MHz proton, 125.7 MHz carbon). The ^1H and ^{13}C assignments were based on gradient enhanced COSY, HMQC, HMBC and DEPT 135. All chemical shifts are recorded in parts per million (ppm), referenced to residual solvent frequencies (^1H NMR: Me_4Si = 0, $CDCl_3$ = 7.26, D_2O = 4.79, CD_3OD = 4.87 or 3.31, DMSO-d_6 = 2.50, Acetone-d_6 = 2.05 and ^{13}C NMR: $CDCl_3$ = 77.16; CD_3OD = 49.0, DMSO-d_6 = 39.5, Acetone-d_6 = 29.9). The following splitting abbreviations were used: s = singlet, d = doublet, t = triplet, q = quartet, p = pentet, m = multiplet, br = broad. High-resolution mass spectra (HRMS) were recorded on a Bruker Q-TOF-2 Micromass spectrometer equipped with lock spray, using ESI with methanol as the carrier solvent. Accurate mass measurements were performed using leucine enkephalin as a lock mass and the data were processed using MassLynx 4.1. Exact *m/z* values are reported in Daltons. Optical rotations were measured on a JASCO P1010 polarimeter at 589 nm (Na D-line) with a path length of 1 dm and are reported with implied units of 10^{-1} deg cm^2 g^{-1}. Concentrations (c) are given in g/100 mL. Melting points (m.p.) were determined using a DigiMelt MPA 160 melting point apparatus and are uncorrected. Infrared (IR) spectra were recorded on a Thermo Nicolet Avatar 360 FT-IR fitted with a Smart Orbit diamond ATR sampler (oils and solids were examined neat). Absorption maxima (ν_{max}) are recorded in wavenumbers (cm^{-1}).

HPLC System and Methods: A Shimadzu Prominence HPLC system equipped with LC-6AD pumps, an autosampler (SIL-20AC) and manual injection port (Rheodyne, 3725i), a column oven (CTO-20A, temperature set at 27 °C), a photo diode array detector (SPD-M20A, using a Deuterium lamp and a tungsten lamp as light sources) and a system controller (CBM-20A) was used in the stability study of BGA and BGG. A post-column adjustable flow splitters (American Scientific Instruments, 600-PO20-03, 20:1splite ratio) and a fraction collector (FRC-10A) were used for preparative purification of final synthetic compounds. The HPLC data were processed using LabSolutions Lite software (version 5.22). Analytical chromatographic separation was carried out by a Phenomenex Kinetex C18 reversed phase column (5 µm, 100 Å, 250 × 4.6 mm) fitted with a guard cartridge, 50 µL per injection was loaded onto the column

and elution was performed with a flow rate of 1.0 mL/min. Preparative purification was carried out using a Phenomenex Kinetex C18 reversed phase column (5 µm, 100 Å, 250 × 21.1 mm) fitted with a guard guard cartridge. Elution was performed with a flow rate of 10.0 mL/min. A gradient of CH_3CN and water was used for the separation of BGG: 0 min, 5% CH_3CN; 5 min, 10% CH_3CN; 10 min, 15% CH_3CN; 12.5 min, 100% CH_3CN. Likewise, BGA was purified using a gradient of acetonitrile/water: 0 min, 0% CH_3CN; 5 min, 2% CH_3CN; 10 min, 5% CH_3CN; 15 min, 100% CH_3CN.

The acidic degradation studies were performed by mixing 100 µL of a 10 mM BGG or BGA solution with 900 µL aqueous H_2SO_4 solution (pH = 0.33) at room temperature and by heating in an oil bath set at 80 °C. The linearity test solutions of BGG and BGA were prepared using concentrations of 50, 100, 200, 500 and 1000 µM. Solution aliquots (50 µL) were analyzed by HPLC to generate calibration curves by plotting the peak area under 254 nm against concentration. The concentrations of BGG or BGA in all degradation studies were determined by the peak area using the calibration curves, and the percentage of remaining compounds were calculated by normalizing them to control samples at initial concentrations. All experiments were performed in triplicate and mean data and standard deviations were calculated.

CHEMICAL SYNTHESES

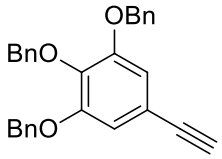

(3,4,5-Tribenzyloxy)phenyl acetylene (13). To a stirred solution of (3,4,5-tribenzyloxy)benzaldehyde[1] (456.8 mg, 1.07 mmol) and K_2CO_3 (295.8 mg, 2.14 mmol) in CH_2Cl_2/CH_3OH (6 mL, v/v, 1:1) at 0 °C was added a solution of dimethyl-1-diazo-2 oxopropyl-phosphonate[2] (513.9 mg, 2.68 mmol) in CH_3OH (3 mL) dropwise. The reaction mixture was allowed to warm to room temperature and stirred for 24 h. The reaction mixture was concentrated to remove CH_3OH, dissolved in CH_2Cl_2, and washed with 1N HCl and brine. The organic layer was dried over Na_2SO_4 and concentrated. Chromatographic purification on silica gel (5% ethyl acetate in hexane) afforded **13** (383.5 mg, 0.912 mmol, 85%). White solid; M.p. 130 °C; IR (neat) ν_{max} 3268, 3064, 3029, 2924, 2862, 2117,1579, 1497, 1231 cm^{-1}; TLC (20% ethyl acetate in hexane) R_f = 0.58; ^1H NMR (500 MHz, $CDCl_3$) δ 7.41–7.25 (m, 15H), 6.80 (s, 2H), 5.07(s, 4H), 5.06 (s, 2H), 3.00 (s, 1H); ^{13}C NMR (125.7 MHz, $CDCl_3$) δ 152.8, 137.7, 136.9, 128.7, 128.3, 128.1, 128.0, 127.6, 117.2, 112.0, 104.9, 83.8, 76.5, 75.4, 71.4; ESI-HRMS calcd. for $C_{29}H_{24}O_3Na$ $[M + Na]^+$ 443.1618, found 443.1633.

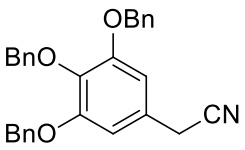

3,4,5-Tribenzyloxybenzyl cyanide. To a stirred solution of (3,4,5-tribenzyloxy) benzyl alcohol[3] (3.22 g, 7.54 mmol) in CH_2Cl_2 (15 mL) at 0 °C was added catalytic amount of DMF (100 μL) followed by $SOCl_2$ (809 μL, 9.81 mmol). The reaction mixture was stirred at 0 °C for 2 h, and then the solvent and excess $SOCl_2$ were removed under reduced pressure to yield the corresponding benzyl chloride. The resulting white solid was dissolved in DMF (20 mL), KCN (1.96 g, 30.2 mmol) and 18-crown-6 (996.5 mg, 3.77 mmol) were added in one portion. The reaction mixture was stirred at room temperature for 16 h, concentrated, dissolved in ethyl acetate, and washed with saturated $NaHCO_3$. The aqueous phase was extracted with ethyl acetate three times, and the combined organic extracts was dried over Na_2SO_4, filtered and concentrated. The residue was recrystallized from CH_3OH to give the cyanide as a white crystalline solid (2.80 g, 6.43 mmol, 85%). M.p. 93–94 °C; IR (neat) ν_{max} 3029, 2934, 2240, 1593, 1503, 1443, 1119 cm^{-1}; TLC (20% ethyl acetate in hexane) R_f = 0.20; ^1H NMR (500 MHz, $CDCl_3$) δ 7.41–7.22 (m, 15H), 6.57 (s, 2H), 5.08 (s, 4H), 5.04 (s, 2H), 3.59 (s, 2H); ^{13}C NMR (125.7 MHz, $CDCl_3$) δ 153.3, 138.1, 137.7, 136.8, 128.7, 128.7, 128.3, 128.1, 128.0, 127.5, 125.4, 117.9, 107.6, 75.3, 71.4, 23.8; ESI-HRMS calcd. for $C_{29}H_{25}NO_3Na$ $[M + Na]^+$ 458.1727, found 458.1731.

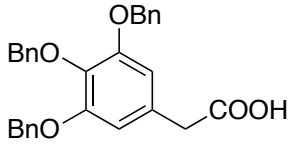

3,4,5-Tribenzyloxyphenylacetic acid (23). To a stirred solution of 3,4,5-tribenzyloxybenzyl cyanide (1.06 mg, 2.43 mmol) in EtOH (5 mL) was added water (5 mL) and KOH (682.8 mg, 12.2 mmol). The reaction mixture was heated to reflux for 20 h and then cooled to room temperature. The reaction mixture was concentrated to remove EtOH, dissolved in CH_2Cl_2, and washed with 1N HCl and brine. The organic extracts was dried over Na_2SO_4 and concentrated. The residue was recrystallized from CH_3OH to give **23** as a white crystalline solid (940 g, 2.08 mmol, 85%). White solid; M.p. 113 °C; IR (neat) ν_{max} 3394, 3030, 2950, 2874, 1708, 1591, 1439, 1372 cm^{-1}; TLC (35% ethyl acetate in hexane) R_f = 0.45; ^1H NMR (500 MHz, $CDCl_3$) δ 7.41–7.25 (m, 15H), 6.60 (s, 2H), 5.08 (s, 4H), 5.02 (s, 2H), 3.53 (s, 2H); ^{13}C NMR (125.7 MHz, $CDCl_3$) δ 177.7, 153.0, 138.04, 137.97, 137.1, 128.8, 128.65, 128.59, 128.3, 128.0, 127.9, 127.6, 109.3, 75.4, 71.4, 41.3; ESI-HRMS calcd. for $C_{29}H_{26}O_5Na$ $[M + Na]^+$ 477.1672, found 477.1665.

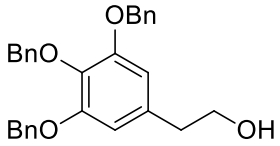

2-(3,4,5-Tribenzyloxyphenyl)ethyl alcohol (15). To a stirred solution of **23** (417.0 mg, 0.917 mmol) in THF (5 mL) at 0 ºC was added $LiAlH_4$ (76.7 mg, 2.02 mmol) portion wise. After 15 min, the cooling bath was removed, and the reaction mixture was stirred at room temperature for 4 h. The reaction mixture was again cooled to 0 ºC, before water was added drop wise to quench the reaction. The reaction mixture was then diluted with CH_2Cl_2 and washed with 1N HCl and brine. The organic layer was dried over Na_2SO_4 and concentrated. Chromatographic purification on silica gel (35% ethyl acetate in hexane) afforded **15** (337.3 mg, 0.766 mmol, 83%). White solid; M.p. 68 °C; IR (neat) ν_{max} 3394, 3064, 3029, 2916, 2864, 1590, 1505, 1431, 1123 cm^{-1}; TLC (35% ethyl acetate in hexane) R_f = 0.23; ^1H NMR (500 MHz, $CDCl_3$) δ 7.43–7.20 (m, 15H), 6.49 (s, 2H), 5.08 (s, 4H), 5.03 (s, 2H), 3.74 (t, *J* = 0.5 Hz, 2H), 2.71 (t, *J* = 0.5 Hz, 2H); ^{13}C NMR (125.7 MHz, $CDCl_3$) δ 153.1, 138.2, 137.5, 137.4, 134.5, 128.9, 128.8, 128.4, 128.2, 128.1, 127.8, 109.0, 75.5, 71.5, 63.8, 39.6; ESI-HRMS calcd. for $C_{29}H_{29}NO_4$ $[M + H]^+$ 441.2060, found 441.2068

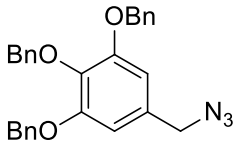

3,4,5-Tribenzyloxybenzyl azide (20). To a stirred solution of (3,4,5-tribenzyloxy)benzyl alcohol[3] (1.50 g, 3.51 mmol) in CH_2Cl_2 (10 ml) at 0 °C was added catalytic amount of DMF (50 μL) followed by $SOCl_2$ (376 μL, 4.57 mmol). The reaction mixture was stirred at 0 °C for 2 h, and then the solvent and excess $SOCl_2$ were removed under reduced pressure to yield the corresponding benzyl chloride. The resulting white solid was dissolved in DMF (10 ml), NaN_3 (456.4 mg, 7.02 mmol) was added in one portion. The reaction mixture was stirred at room temperature for 6 h. The reaction mixture was concentrated, dissolved in ethyl acetate, and washed with saturated $NaHCO_3$. The aqueous phase was extracted with ethyl acetate three times, and the combined organic phase was dried over Na_2SO_4, filtered and concentrated. Chromatographic purification on silica gel (5% ethyl acetate in hexane) provided **20** (1.49 g, 3.30 mmol) in 94% yield. White solid; M.p. 71–72 °C; IR (neat) ν_{max} 3066, 3029, 2932, 2870, 2081, 1590, 1501, 1437, 1126 cm^{-1}; TLC (20% ethyl acetate in hexane) R_f = 0.50; ^1H NMR (500 MHz, $CDCl_3$) δ 7.42–7.22 (m, 15H), 6.60 (s, 2H), 5.10 (s, 4H), 5.05 (s, 2H), 4.20 (s, 2H);^{13}C NMR (125.7 MHz, $CDCl_3$) δ 153.2, 138.5, 137.9, 137.0, 131.1, 128.7, 128.6, 128.3, 128.0, 127.9, 127.5, 108.0, 75.3, 71.4, 55.1; ESI-HRMS calcd. for $C_{28}H_{25}N_3O_3Na$ $[M + Na]^+$ 474.1788, found 474.1795.

BIOLOGICAL STUDIES MATERIALS AND METHODS

Activity of AKR 1B1, AKR1B10 and AKR1A1: The aldose reductase family enzymes were prepared according to the methods of Hayman and Kinoshita.[4] Recombinant human aldose reductase (AKR1B1) was purified from *E. coli* host cultures as described previously.[5] Enzyme solutions were stored at −80 °C and thawed from storage one time only and maintained at 4 °C for no longer than 7 days before use. Aldose reductase activity was determined spectrophotometrically by measuring the decrease in absorbance at 340 nm upon oxidation of NADPH. Reaction mixtures in 1.0 ml quartz cuvettes contained 1.0 mM DL-glyceraldehyde, 150 μM NADPH in KAB buffer (50 mM HEPES, pH 7.5, 150 mM NaCl, 1 mM DTT, 10 mM $MgCl_2$). Note: the enzyme, NADPH, and DL-glyceraldehyde were maintained on ice and the buffer and water solutions were maintained at rt. Prior to reaction initiation the assay components were combined at rt and reactions were initiated by addition of enzyme to a final concentration of 0.1-0.5 μM and the assay temperature was maintained at 37 °C with a peltier temperature-controlling device fitted to the cuvette transporter. Experimental rates were corrected for background (blank) rates obtained using reaction mixtures containing all components except enzyme. When appropriate, inhibitors were added to reaction mixtures before enzyme was added. Reaction rates were computed from absorbance changes recorded over a period of 5 min. For kinetics studies, rates were measured in triplicate under varying substrate and/or inhibitor concentrations.

Sorbitol colometric assay: Sorbitol accumulation was measured using a previously described method.[6] Briefly, Raw264.7 murine macrophage cells (10^7) were cultured in 100 mm tissue culture dishes using standard conditions (humidified incubator containing 5% CO_2 at 37 °C) and treated with BGG derivatives for 24 h. Cells were collected and washed with cold PBS three times, and the cell lysates were deproteinized using a deproteinizing sample preparation kit (BioVision, Milpitas, CA). Sorbitol was then measured using a D-sorbitol colorimetric assay kit as described by the manufacturer (BioVision, Milpitas, CA).

Lens organ culture studies: Sorbitol accumulation was measured as previously described[7] using lenses from wild type and human AKR1B1 overexpressing PAR40 mice which are on a C57BL6 strain background. Lenses were cultured in DMEM (high glucose, 27.5 mM) in the presence or absence of BGG derivatives for 3 days, and sorbitol level was measured using the Sorbitol colometric assay.

MOLECULAR MODELING METHOD

Computational modeling was carried out using Discovery Studio 4.0 (Accelrys Software Inc., http://www.accelrys.com). The CHARMm force field was applied to the 0.66 Å AKR1B1 (PDB id: 1US0) crystal structure, water molecules were removed, and residues were corrected for physiological pH. The receptor was minimized by Smart Minimizer algorithm, an algorithm that performs 1000 steps of Steepest Descent with a root mean square (RMS) gradient tolerance of 3. The binding site was defined as whole residues within a 10 Å radius subset encompassing the active site. All ligands were prepared and typed with CHARMm force field before docking studies. LibDock was used to filter the confirmation of the substrates. The number of specified hotspots was set at 200 and max hits to save was set at 3 for each ligand using the 'BEST' algorithm for conformational sampling. The top poses of each ligand were selected for flexible docking by using the corresponding protocol in DS 4.0 that allows for receptor flexibility. The flexible residues were determined to be those in the anionic pocket (Trp20, Val47, Tyr48, Trp79, His 110, Trp111, Phe115 and Phe122) and specificity pocket (Thr113, Trp219, Val297, Cys298, Ala299, Leu300, Cys303 and Tyr309). Simulated annealing between 300 and 700 K and post-docking ChiRotor refinement were allowed. In addition to binding energies, the top 20 poses (based on –CDOCKER energy) generated for each compound were analyzed and considered.

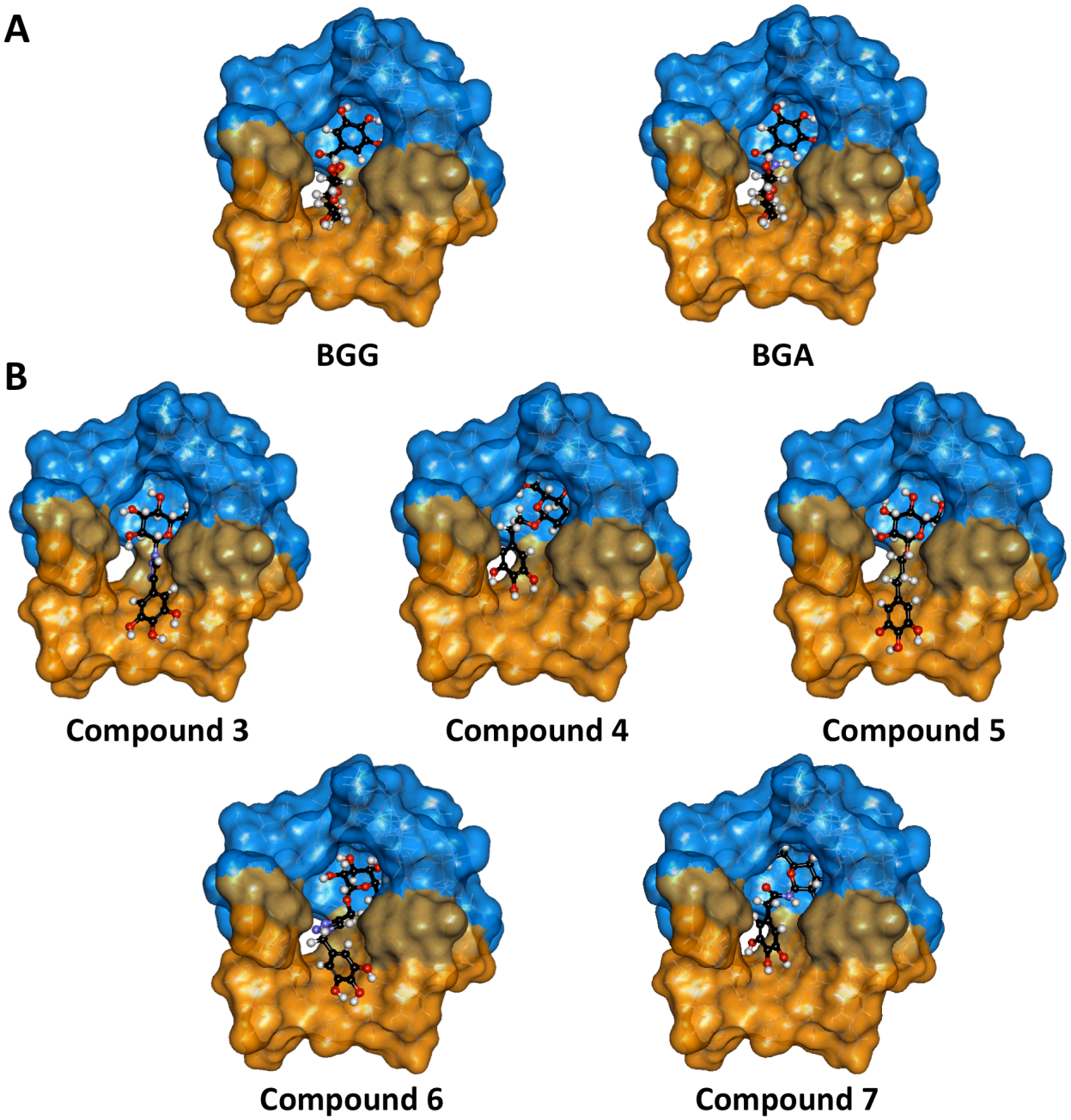

Figure S1. Representative binding poses for BGG, BGA, and compounds **3**–**7** bound to AKR1B1 using the top 20 poses ranked by docking score. (A) A favorable inhibitory binding pose of BGG and BGA is represented with the sugar moiety is positioned in the "anionic" pocket (orange surface) and the gallate ring is positioned in the "specificity" pocket (blue surface). (B) An unfavorable binding pose of compounds **3**–**7**, depicting an opposite configuration to BGG and BGA.

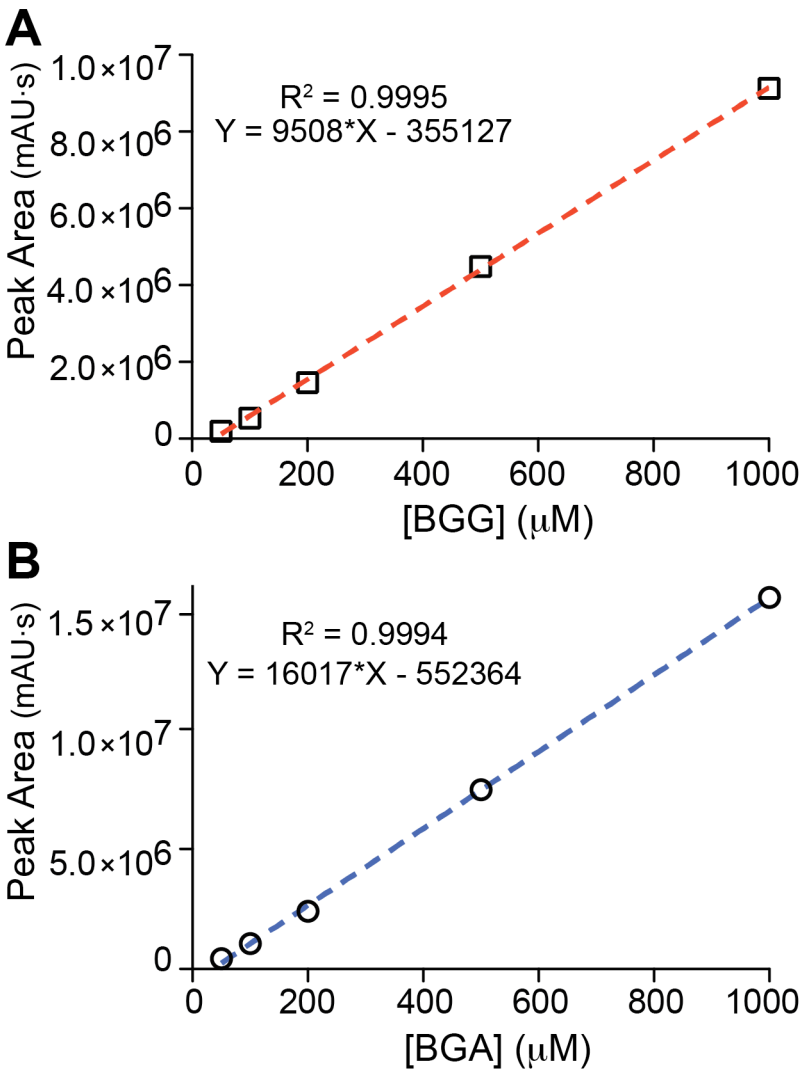

Figure S2. The HPLC concentration calibration curves used to quantitate (**A**) the degradation of of BGG, and (**B**) the stability of BGA.

SUPPORTING INFORMATION REFERENCES

(1) Zhuravel, M. A.; Davis, N. E.; Nguyen, S. T.; Koltover, I. Dendronized protein polymers: Synthesis and self-assembly of monodisperse cylindrical macromolecules. *J. Am. Chem. Soc.* **2004**, *126*, 9882-9883.

(2) Pietruszka, J.; Witt, A. Synthesis of the Bestmann-Ohira reagent. *Synthesis* **2006**, 4266-4268.

(3) Dodo, K.; Minato, T.; Noguchi-Yachide, T.; Suganuma, M.; Hashimoto, Y. Antiproliferative and apoptosis-inducing activities of alkyl gallate and gallamide derivatives related to (-)-epigallocatechin gallate. *Bioorg. Med. Chem.* **2008**, *16*, 7975-7982.

(4) Hayman, S.; Kinoshita, J. H. Isolation and properties of lens aldose reductase. *J. Biol. Chem.* **1965**, *240*, 877-882.

(5) Nakano, T.; Petrash, J. M. Kinetic and spectroscopic evidence for active site inhibition of human aldose reductase. *Biochemistry* **1996**, *35*, 11196-11202.

(6) Chang, K.-C.; Laffin, B.; Ponder, J.; Énzsöly, A.; Németh, J.; LaBarbera, D. V.; Petrash, J. M. Beta-glucogallin reduces the expression of lipopolysaccharide-induced inflammatory markers by inhibition of aldose reductase in murine macrophages and ocular tissues. *Chem. Biol. Interact.* **2013**, *202*, 283-287.

(7) Puppala, M.; Ponder, J.; Suryanarayana, P.; Reddy, G. B.; Petrash, J. M.; LaBarbera, D. V. The isolation and characterization of β-glucogallin as a novel aldose reductase inhibitor from *Emblica officinalis*. *PLoS One* **2012**, *7*, e31399.

2,3,4,6-Tetra-*O*-benzyl-1-*O*-(tri-*O*-benzylgalloyl) β-D-glucopyranose (10)

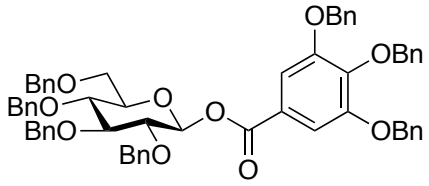

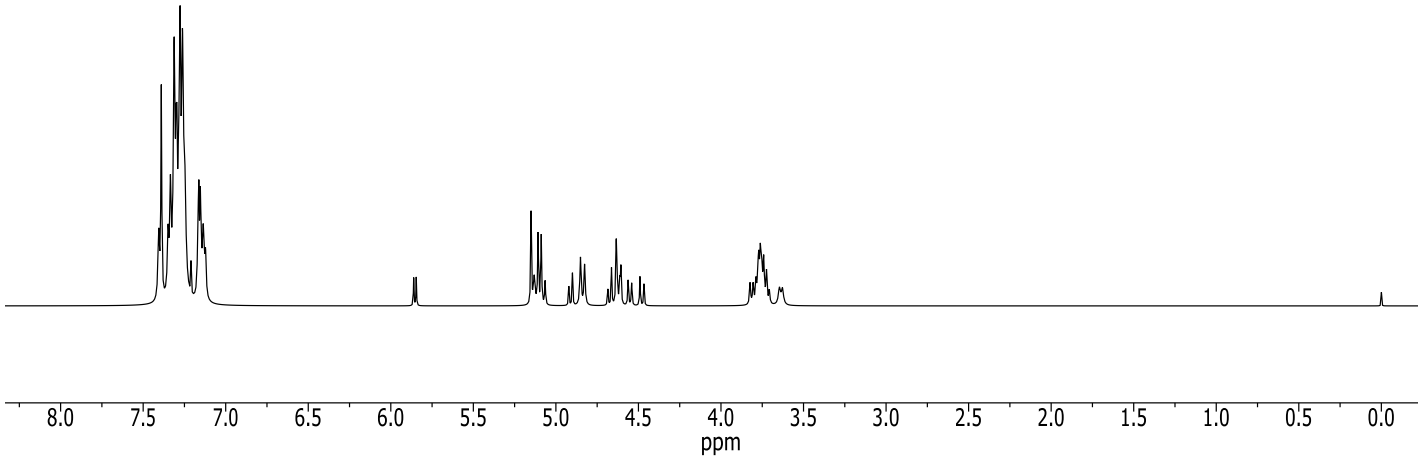

2,3,4,6-Tetra-*O*-benzyl-1-*O*-(tri-*O*-benzylgalloyl) β-D-glucopyranose (10)

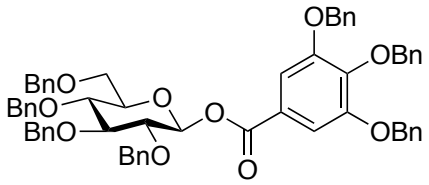

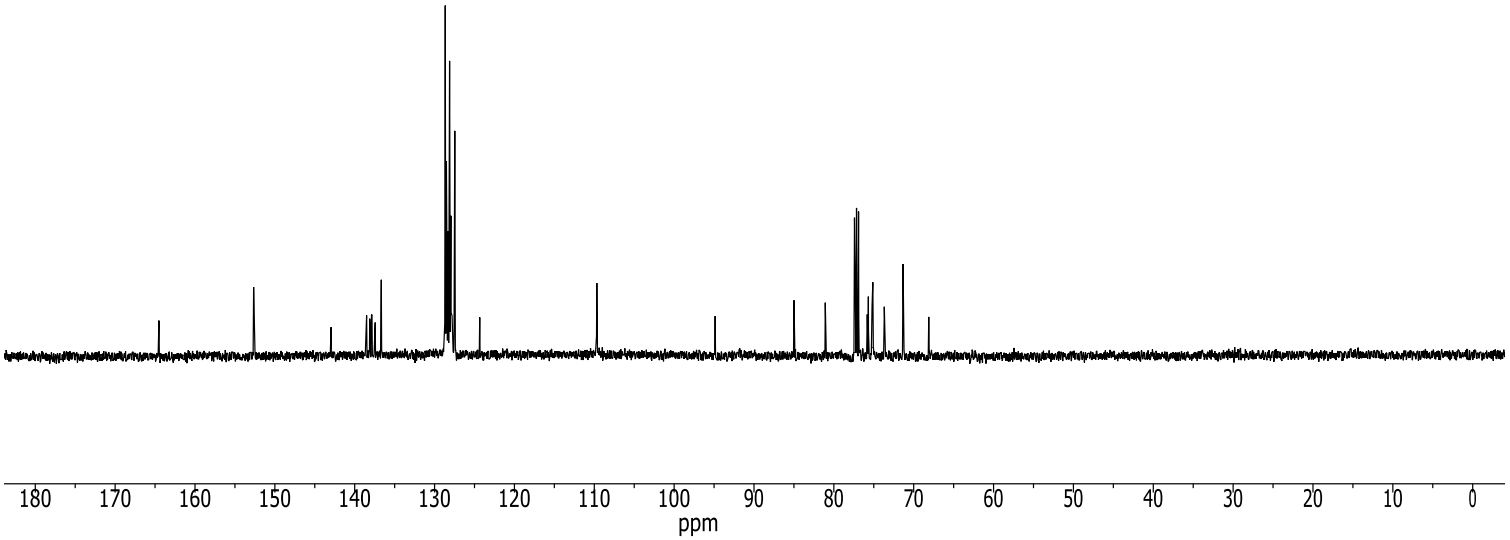

_N_-(3,4,5-Tri-_O_-benzylgalloyl)-2,3,4,6-tetra-_O_-acetyl β-D-glucopyranosylamine (12)

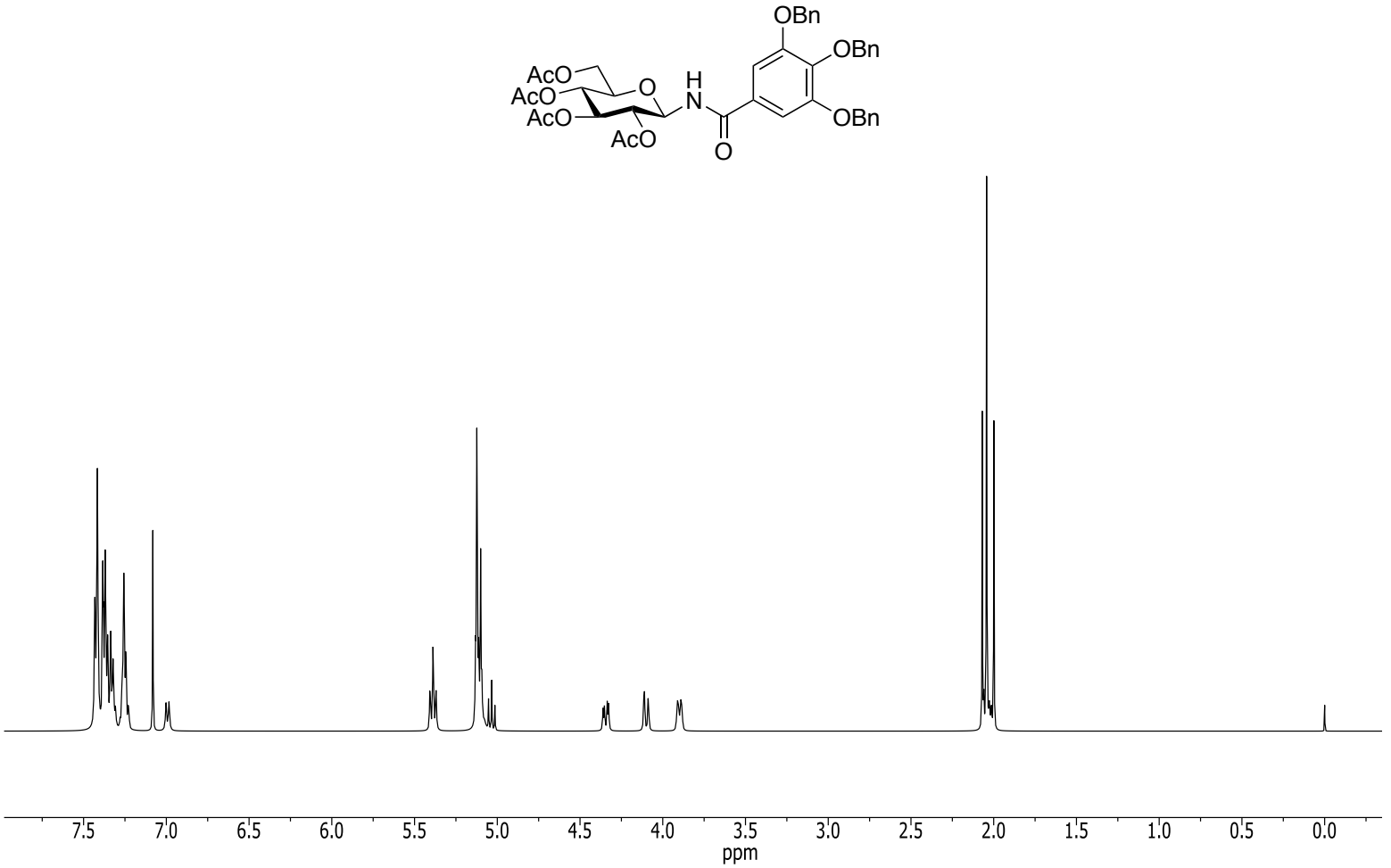

_N_-(3,4,5-Tri-_O_-benzylgalloyl)-2,3,4,6-tetra-_O_-acetyl β-D-glucopyranosylamine (12)

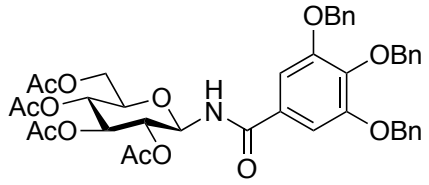

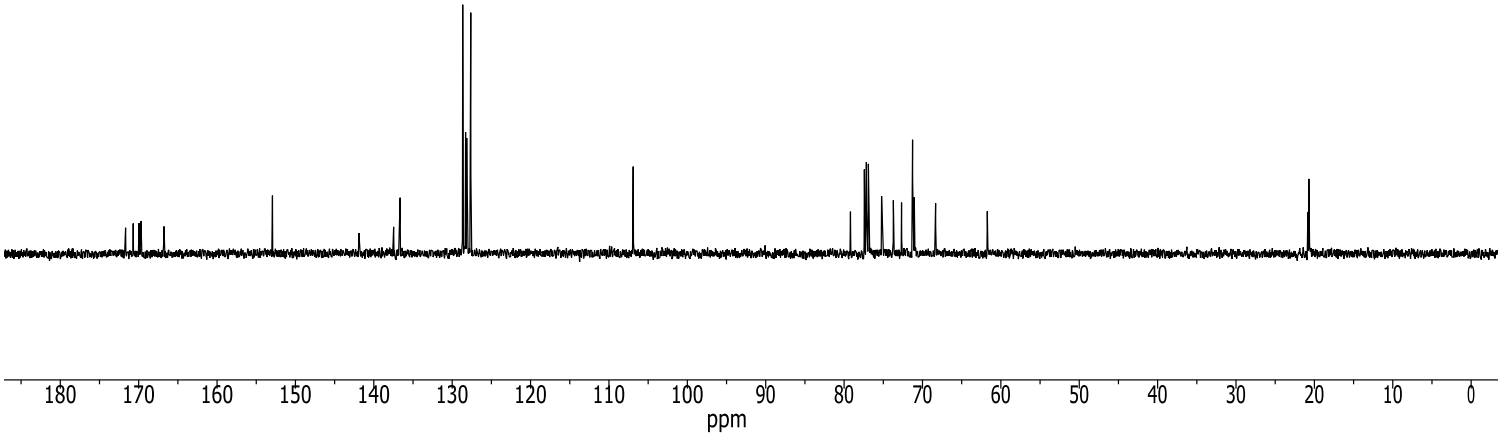

_N_-galloyl β-D-glucopyranosylamine (BGA, 2)

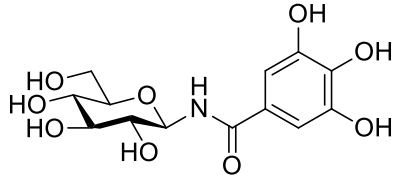

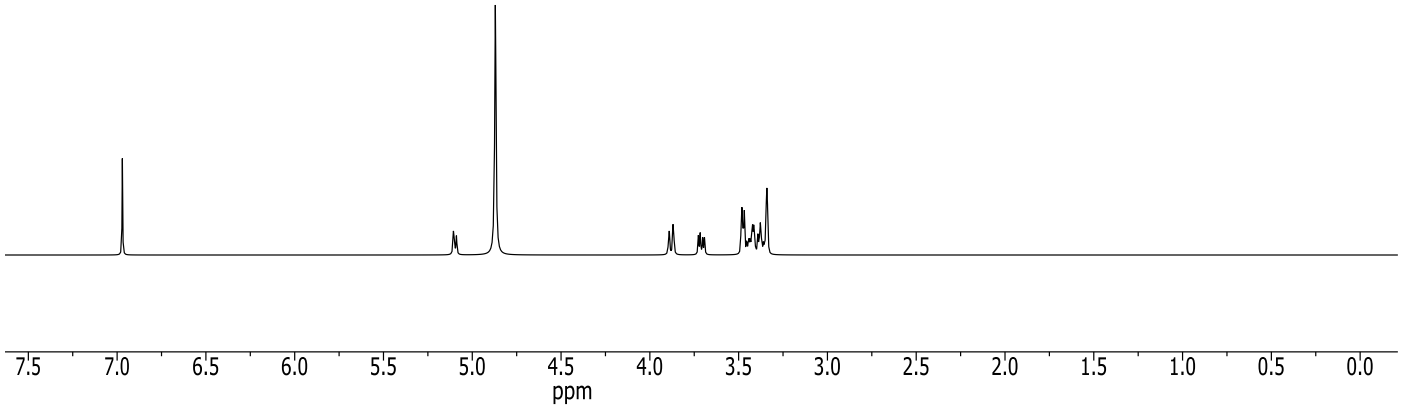

_N_-galloyl β-D-glucopyranosylamine (BGA, 2)

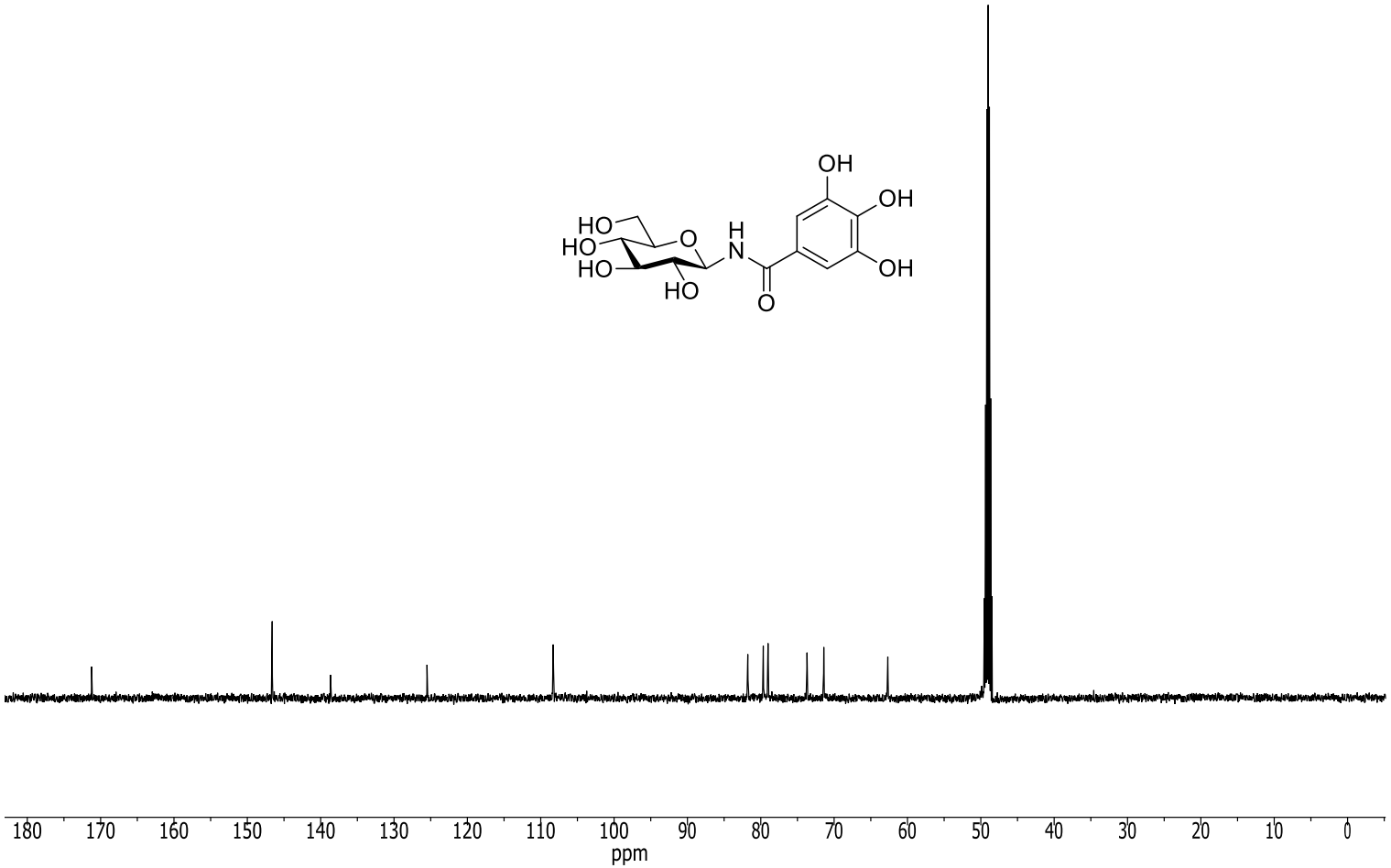

_N_-galloyl β-D-glucopyranosylamine (BGA, 2)

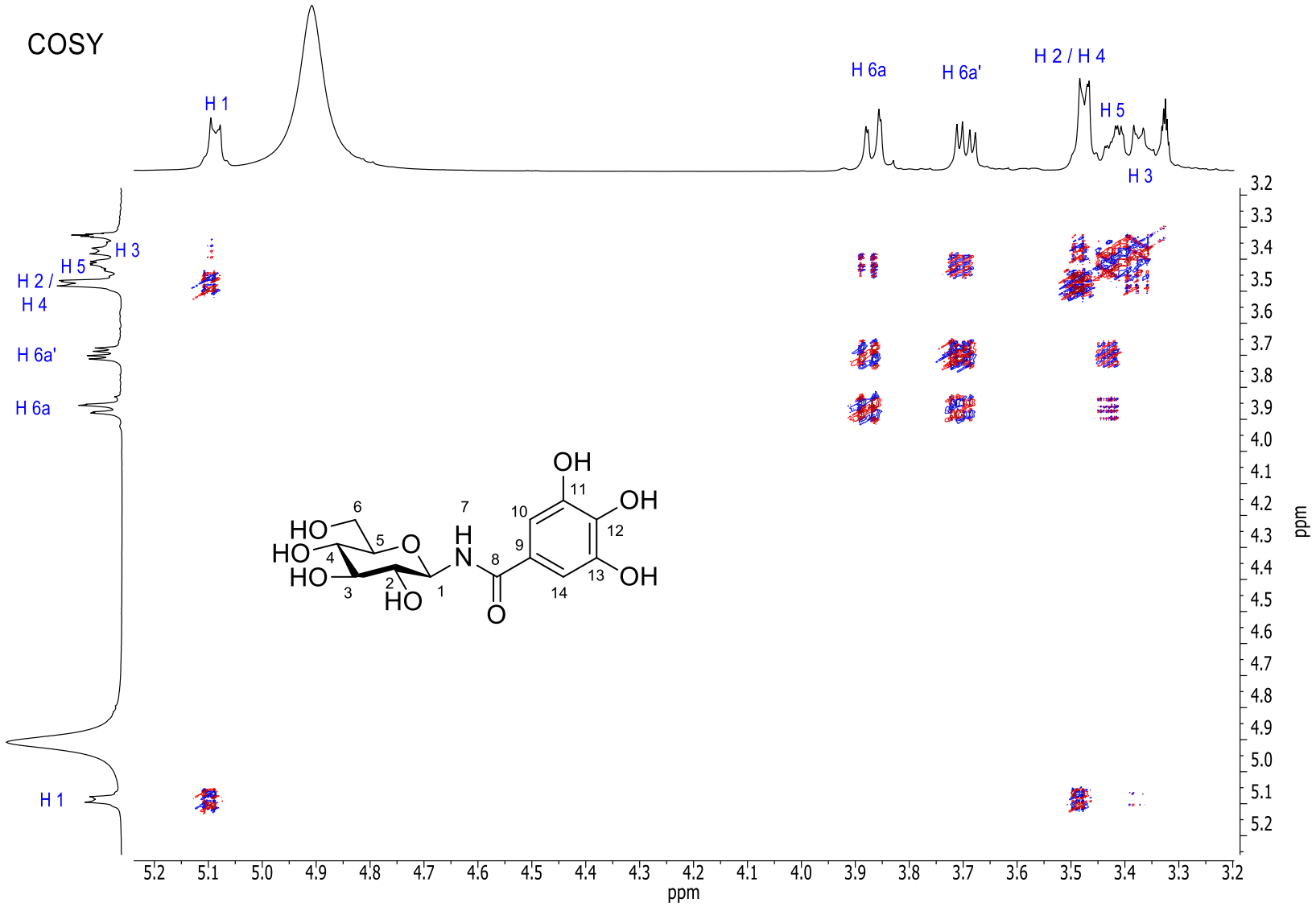

_N_-galloyl β-D-glucopyranosylamine (BGA, 2)

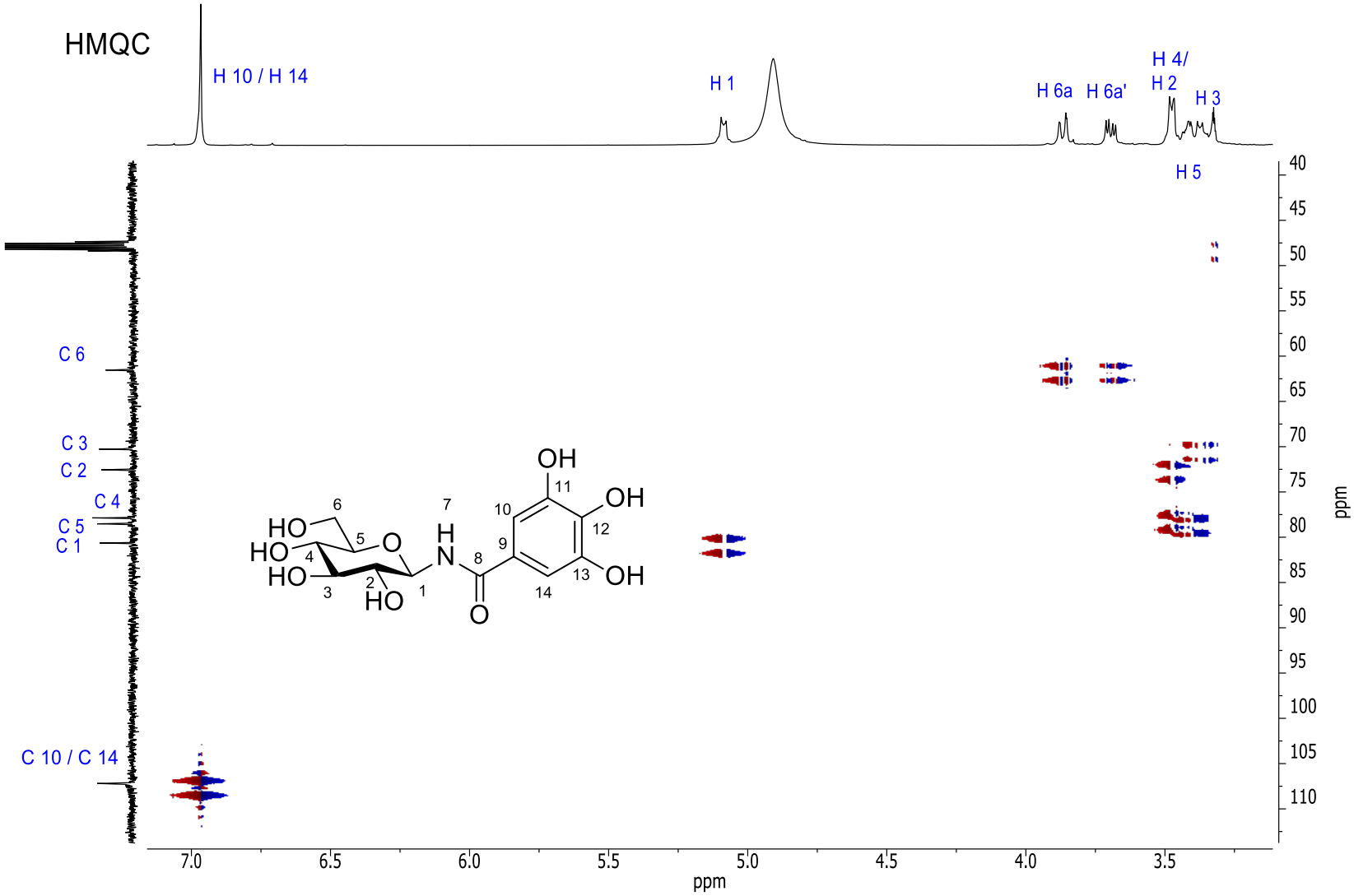

_N_-galloyl β-D-glucopyranosylamine (BGA, 2)

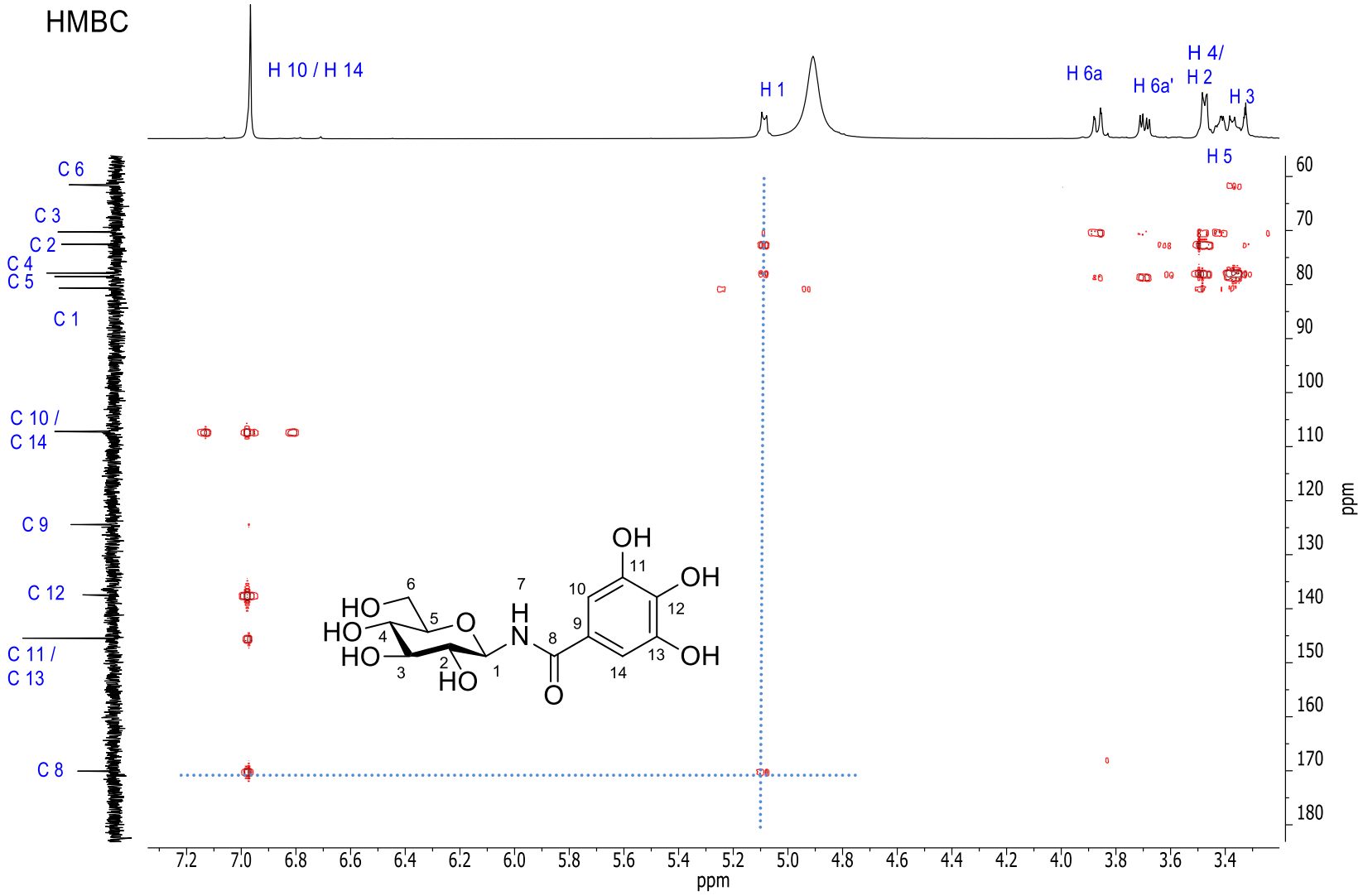

(3,4,5-Tribenzyloxy)phenyl acetylene (13)

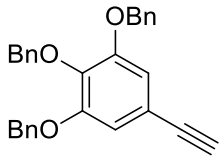

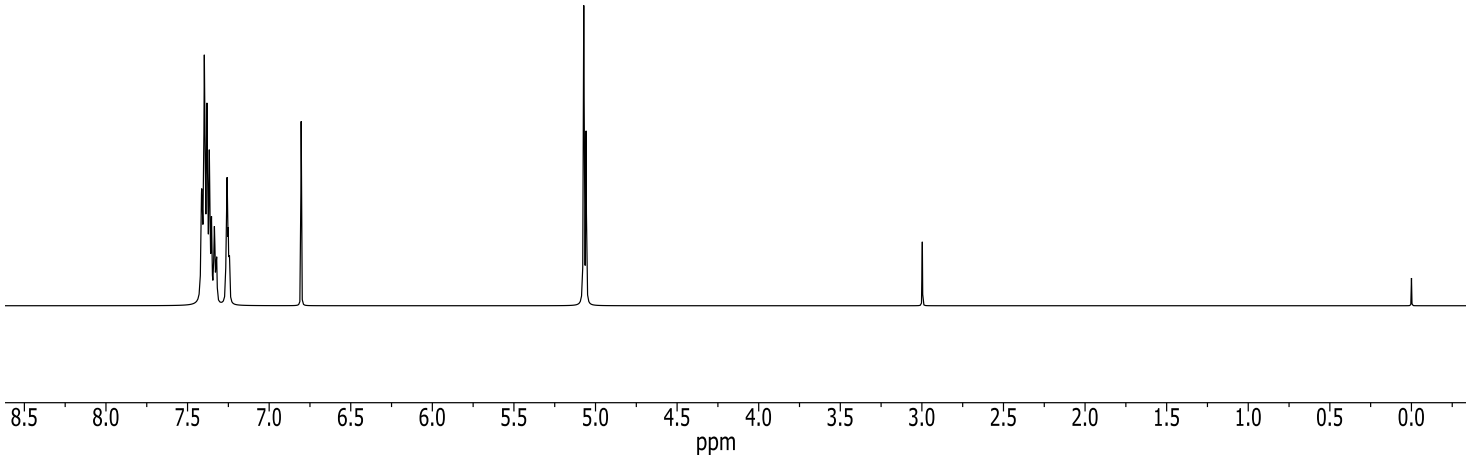

(3,4,5-Tribenzyloxy)phenyl acetylene (13)

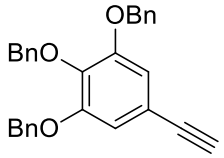

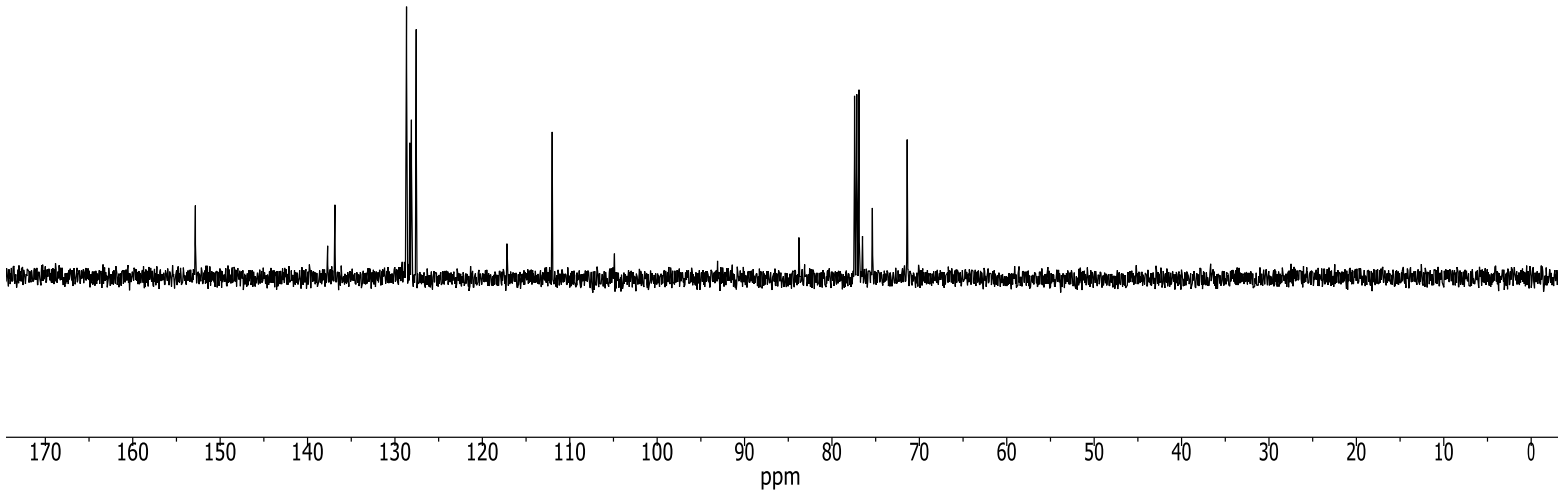

1-(2,3,4,6-Tetra-*O*-acetyl-β-D-glucopyranosyl)-4-(3,4,5-tribenzyloxyphenyl)-1,2,3-triazole (14)

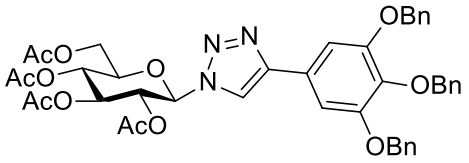

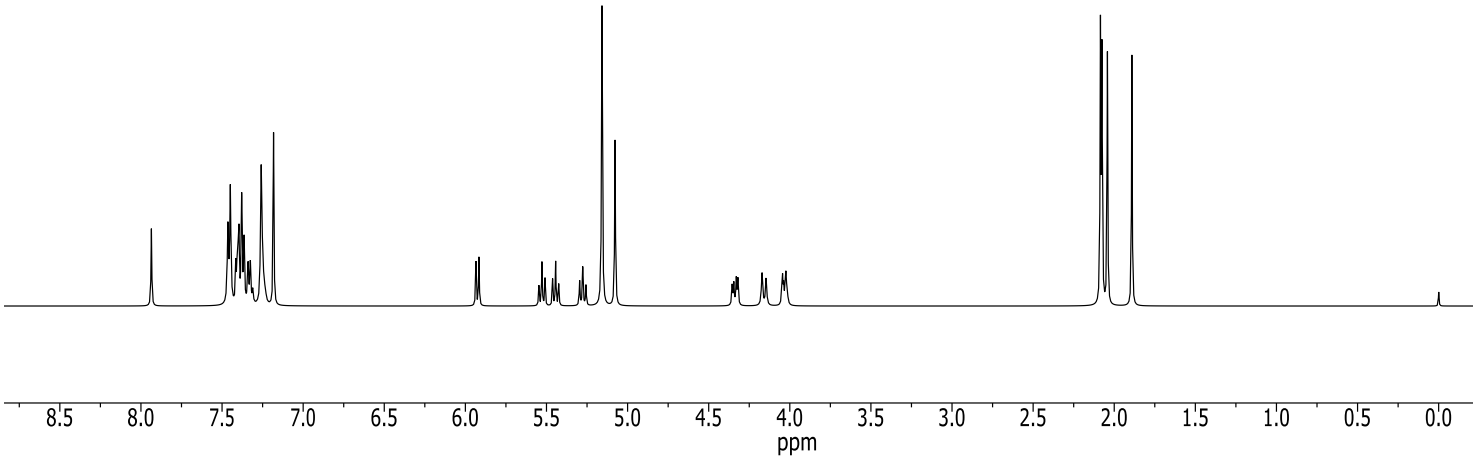

1-(2,3,4,6-Tetra-*O*-acetyl-β-D-glucopyranosyl)-4-(3,4,5-tribenzyloxyphenyl)-1,2,3-triazole (14)

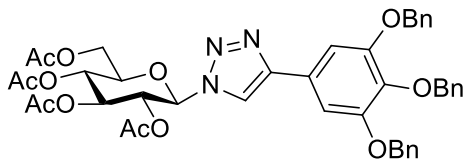

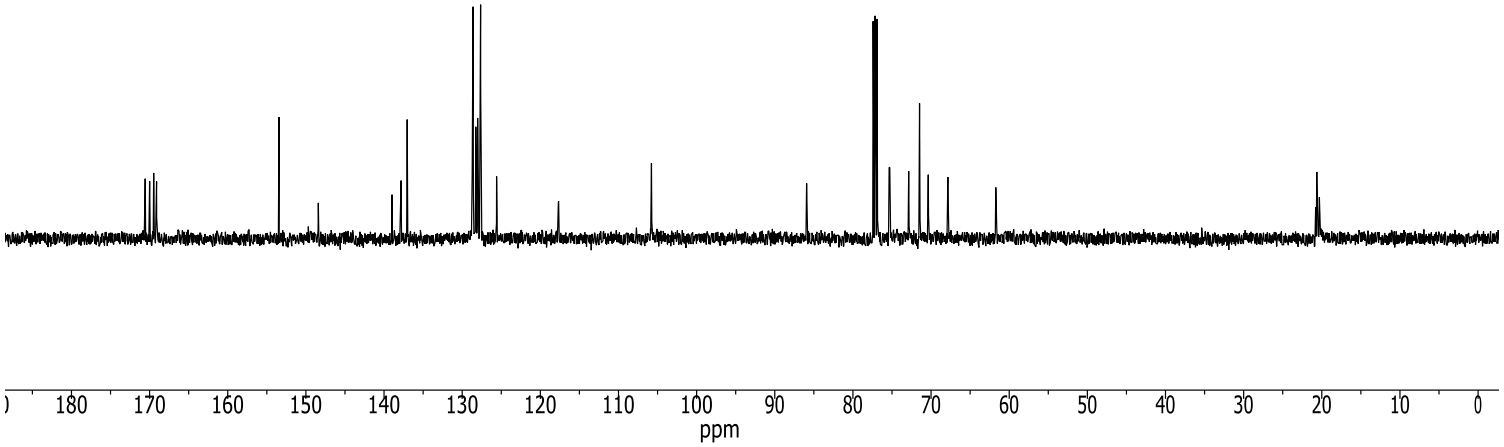

1-(β-D-glucopyranosyl)-4-(3,4,5-trihydroxyphenyl)-1,2,3-triazole (3)

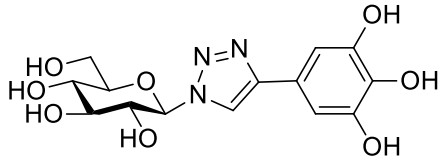

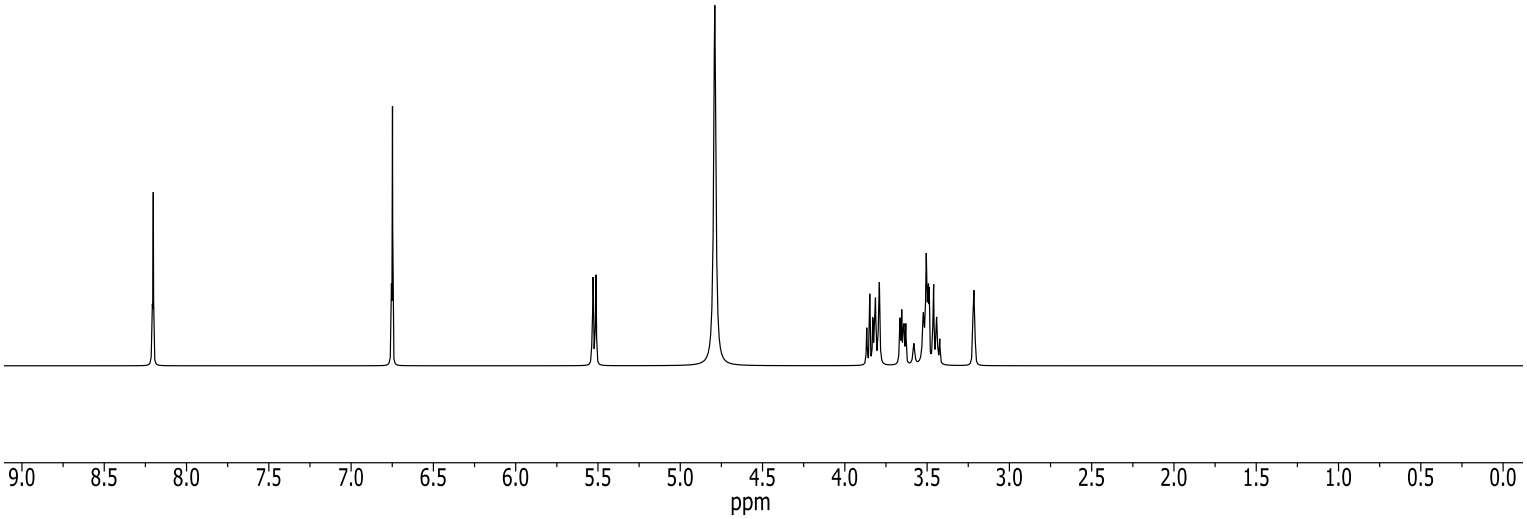

1-(β-D-glucopyranosyl)-4-(3,4,5-trihydroxyphenyl)-1,2,3-triazole (3)

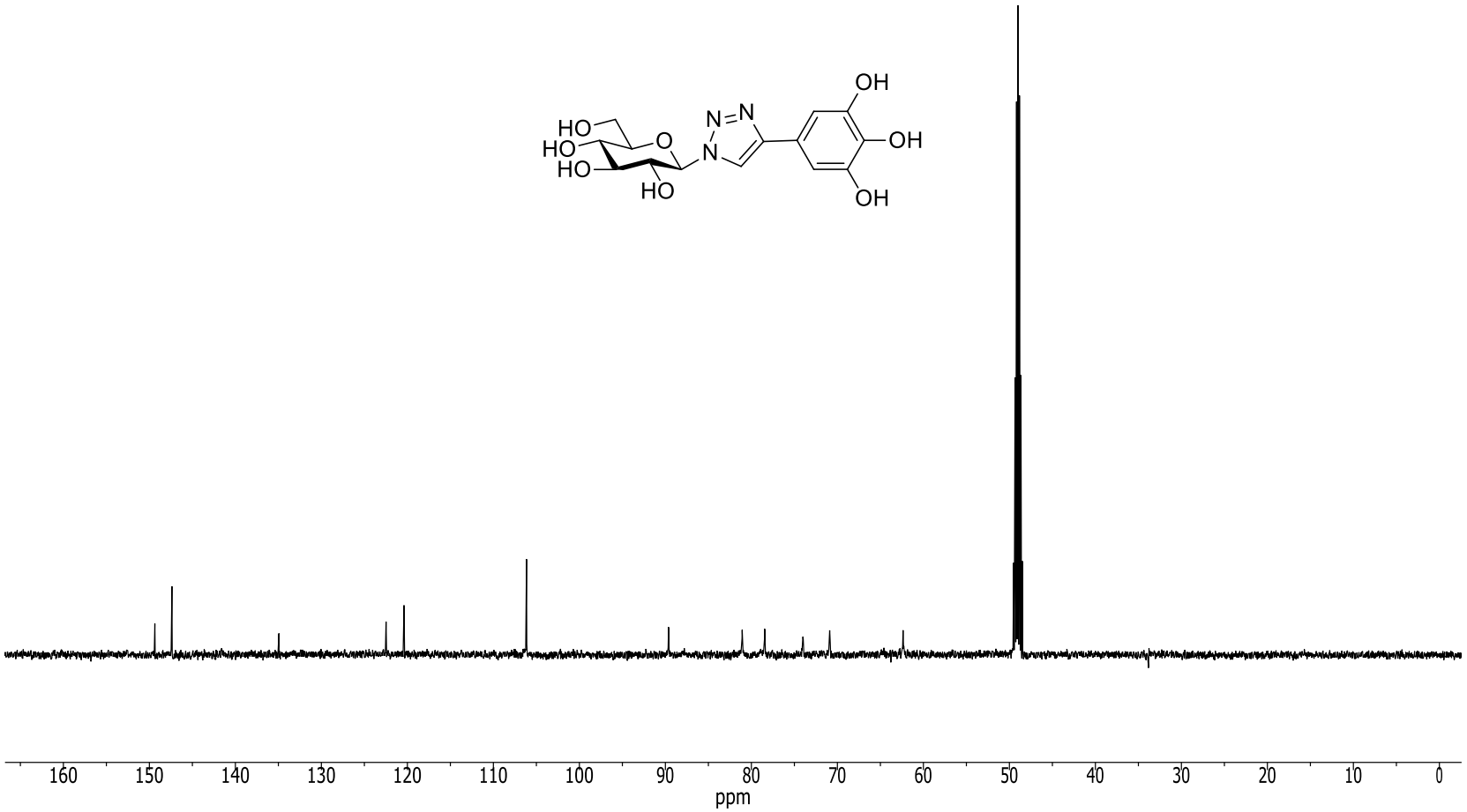

3,4,5-Tribenzyloxybenzyl cyanide

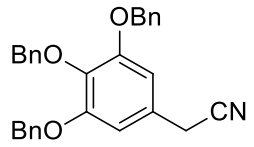

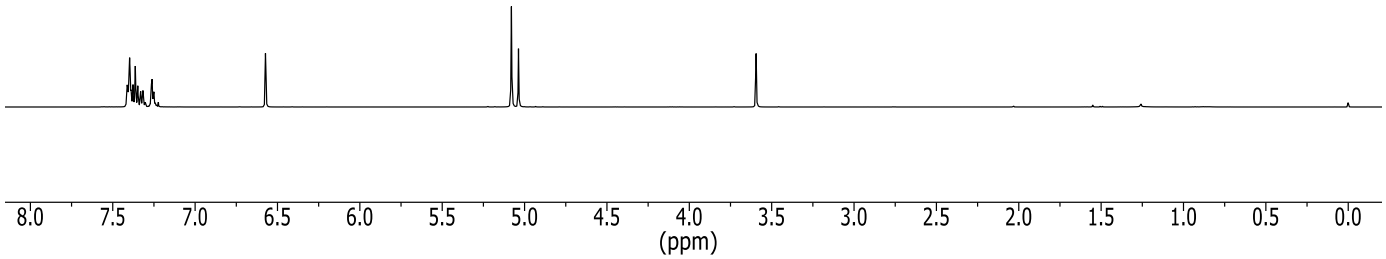

3,4,5-Tribenzyloxybenzyl cyanide

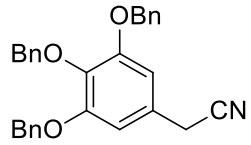

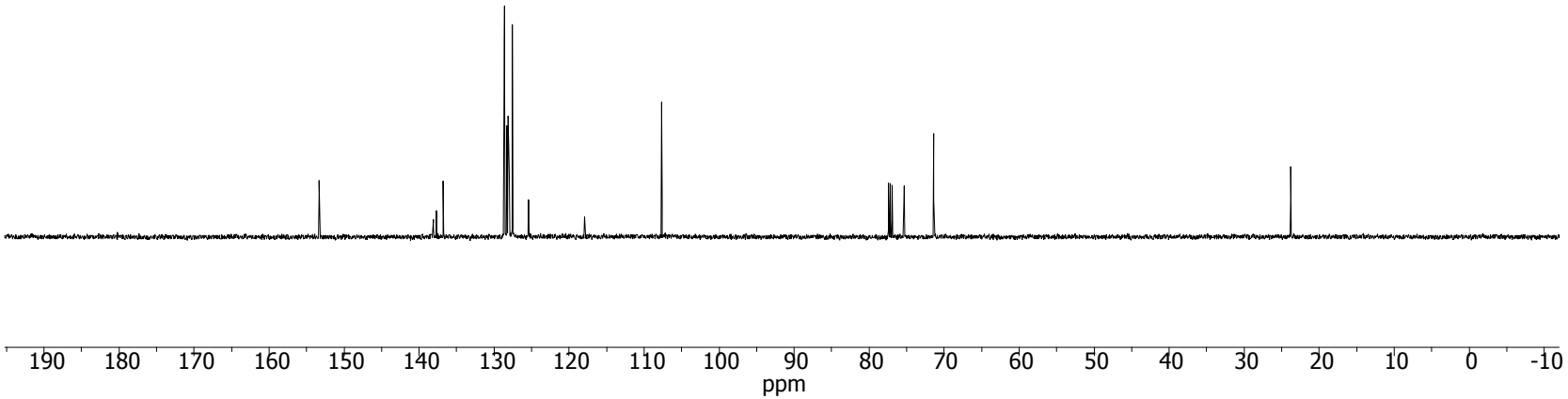

3,4,5-Tribenzyloxyphenylacetic acid (23)

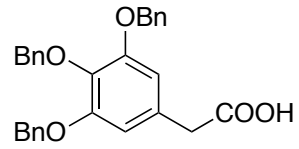

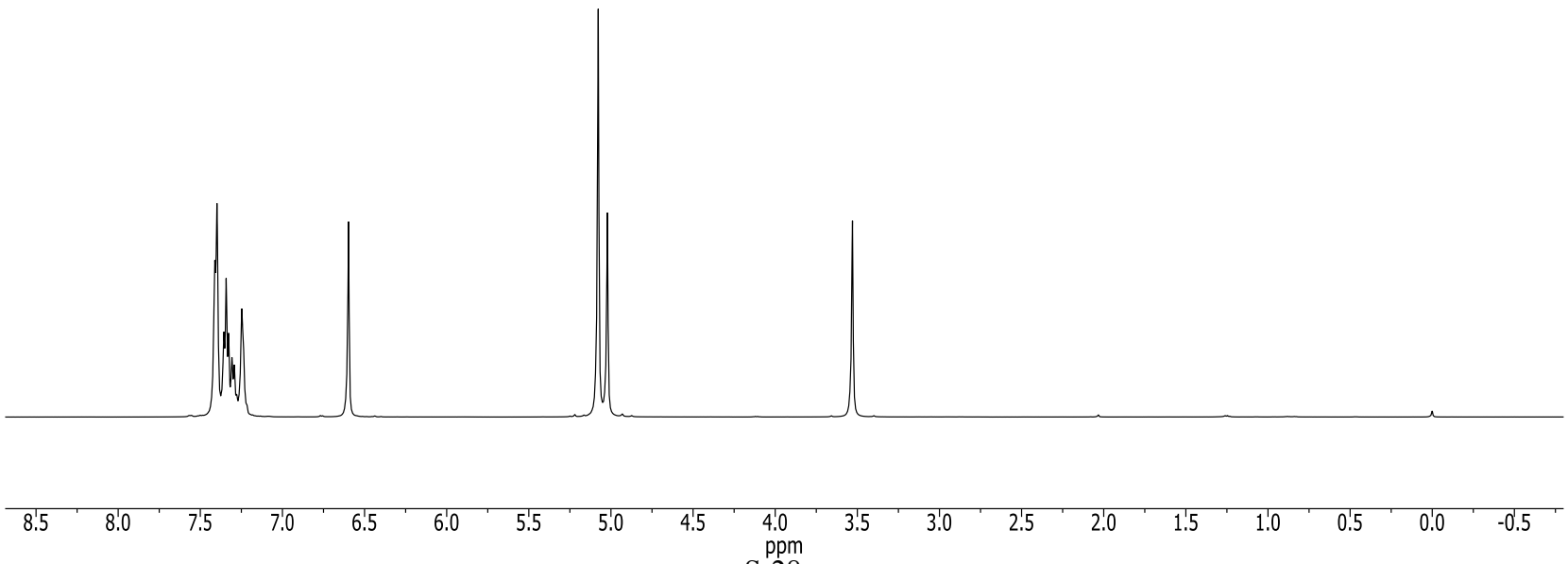

3,4,5-Tribenzyloxyphenylacetic acid (23)

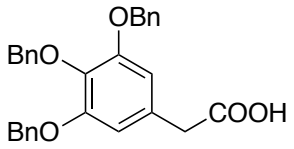

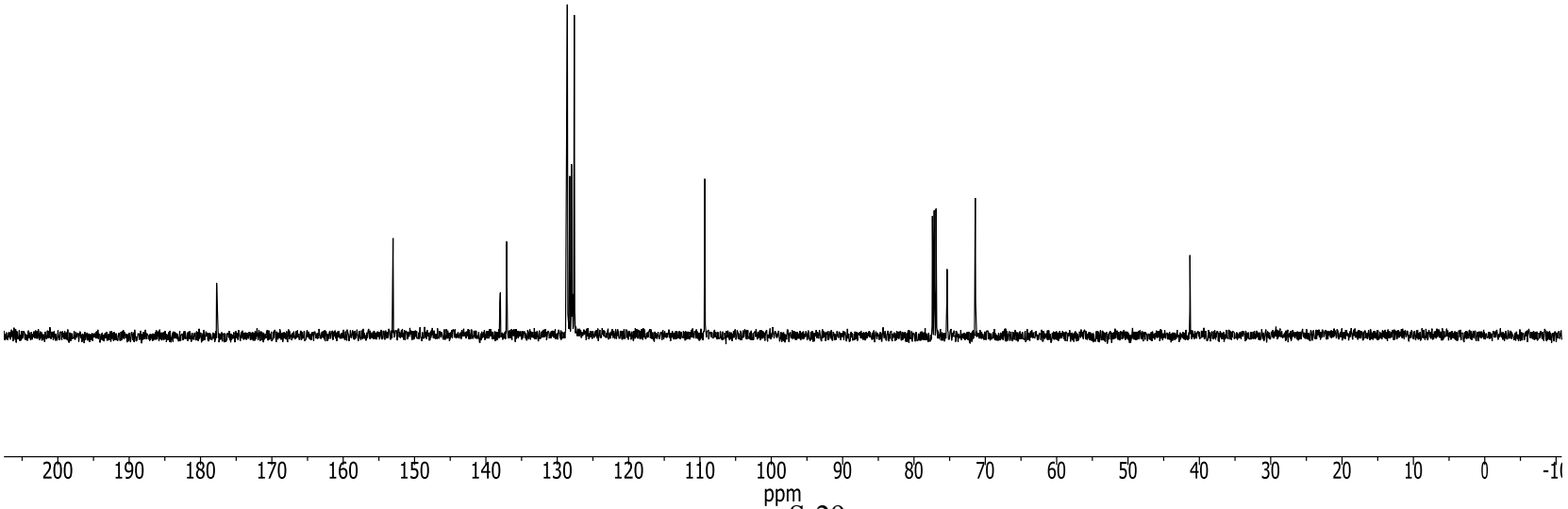

2-(3,4,5-Tribenzyloxyphenyl)ethyl alcohol (15)

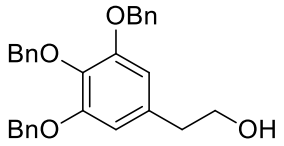

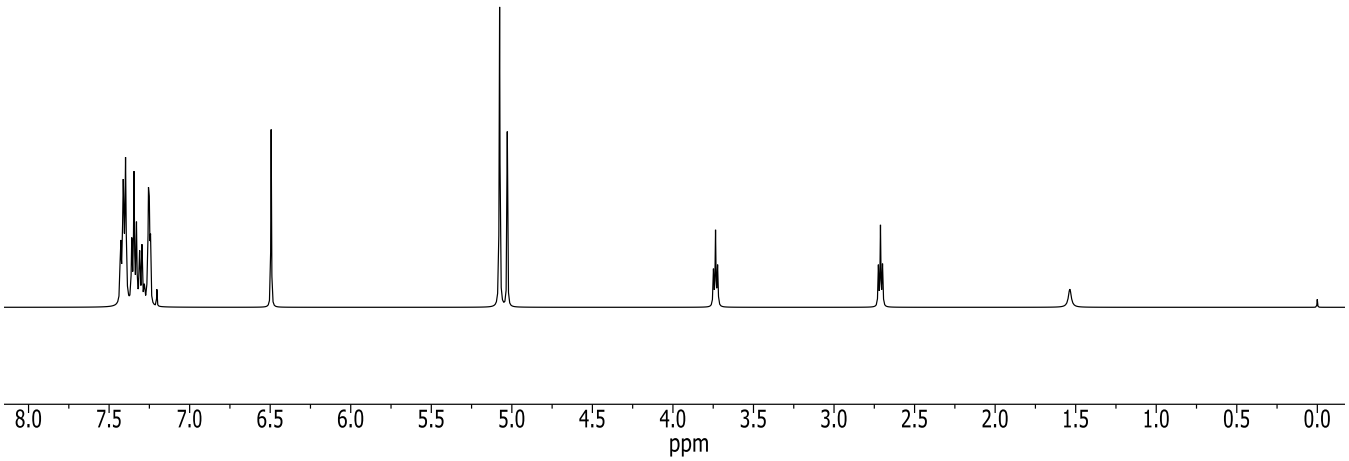

2-(3,4,5-Tribenzyloxyphenyl)ethyl alcohol (15)

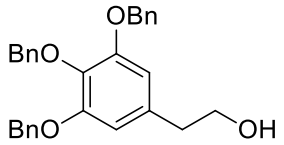

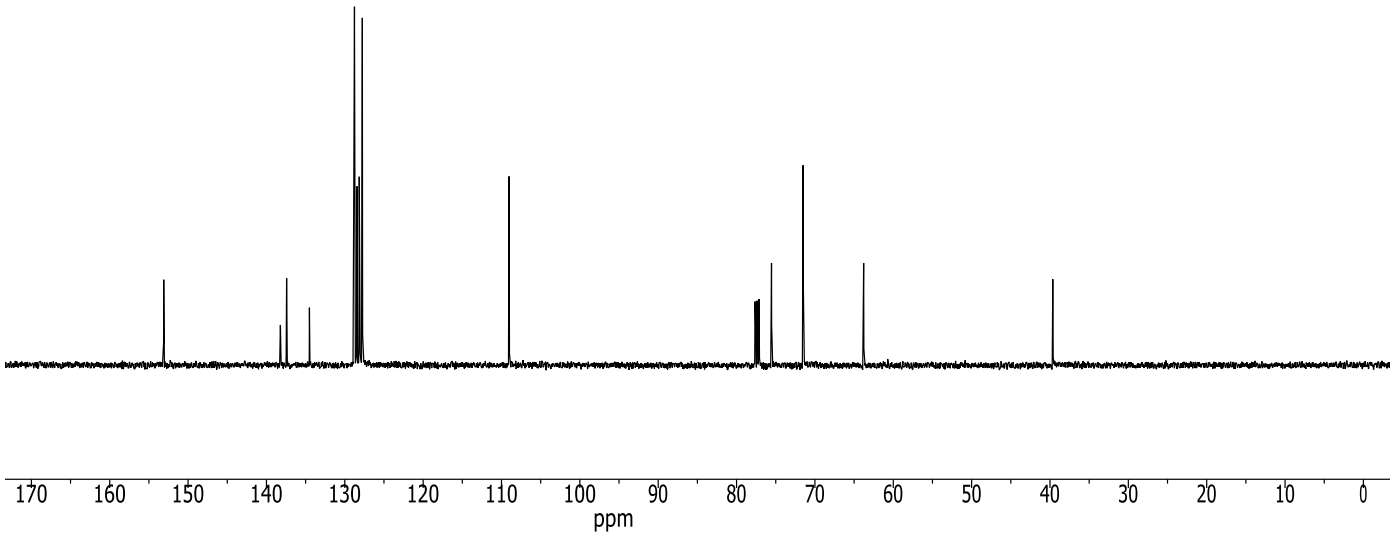

2-(3,4,5-Tribenzyloxyphenyl)ethyl β-D-glucopyranoside (17)

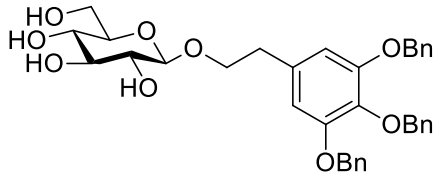

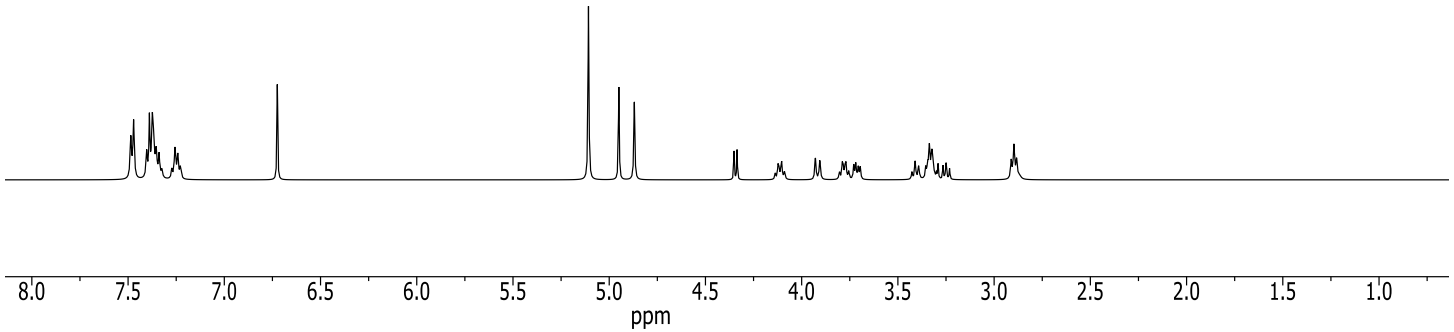

2-(3,4,5-Tribenzyloxyphenyl)ethyl β-D-glucopyranoside (17)

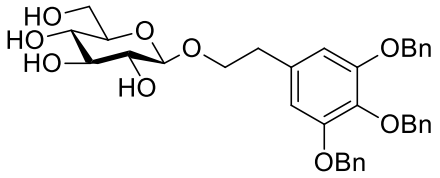

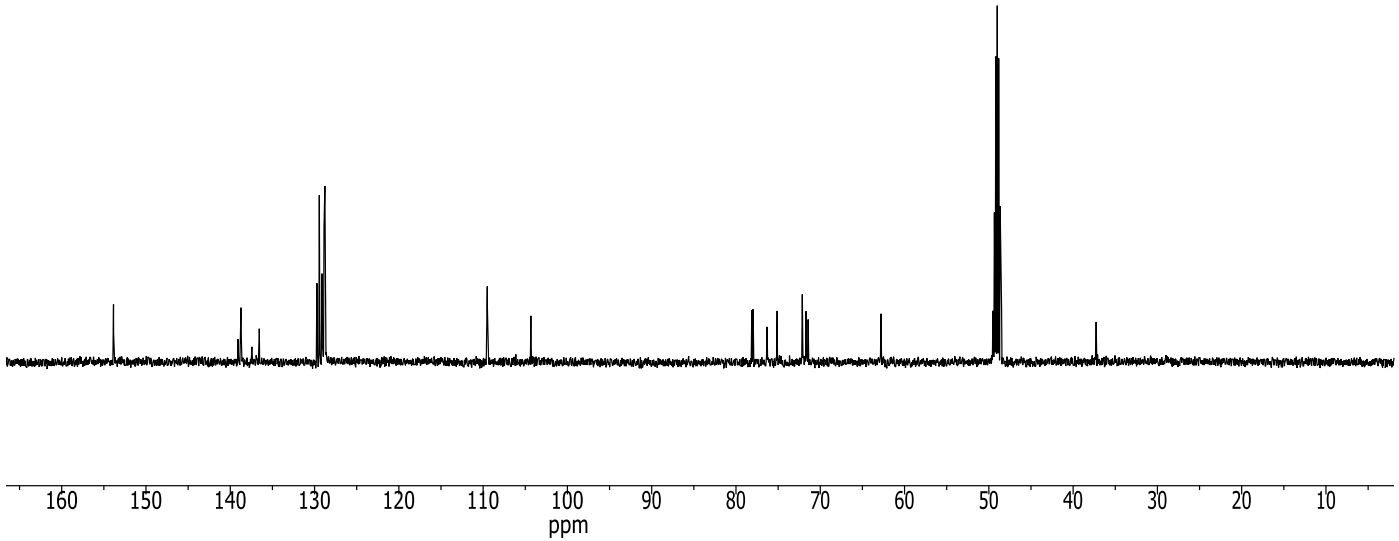

2-(3,4,5-Trihydroxyphenyl)ethyl β-D-glucopyranoside (4)

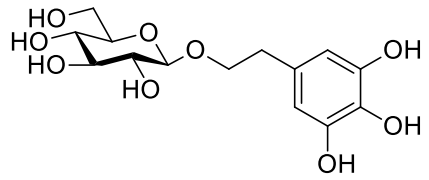

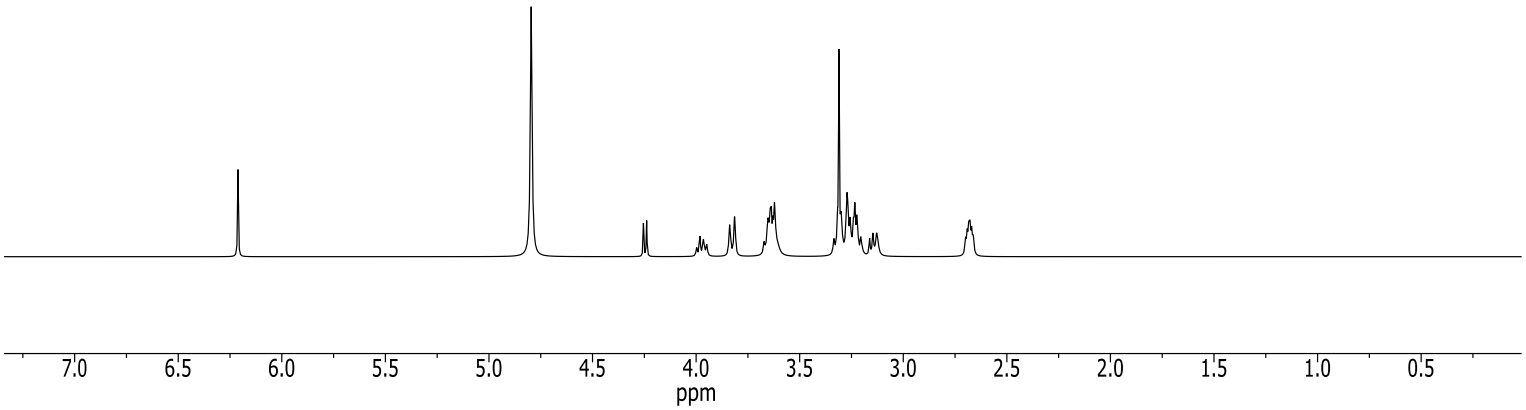

2-(3,4,5-Trihydroxyphenyl)ethyl β-D-glucopyranoside (4)

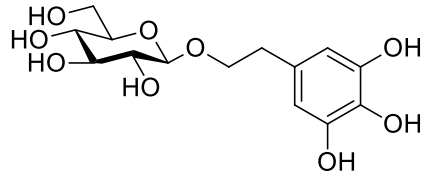

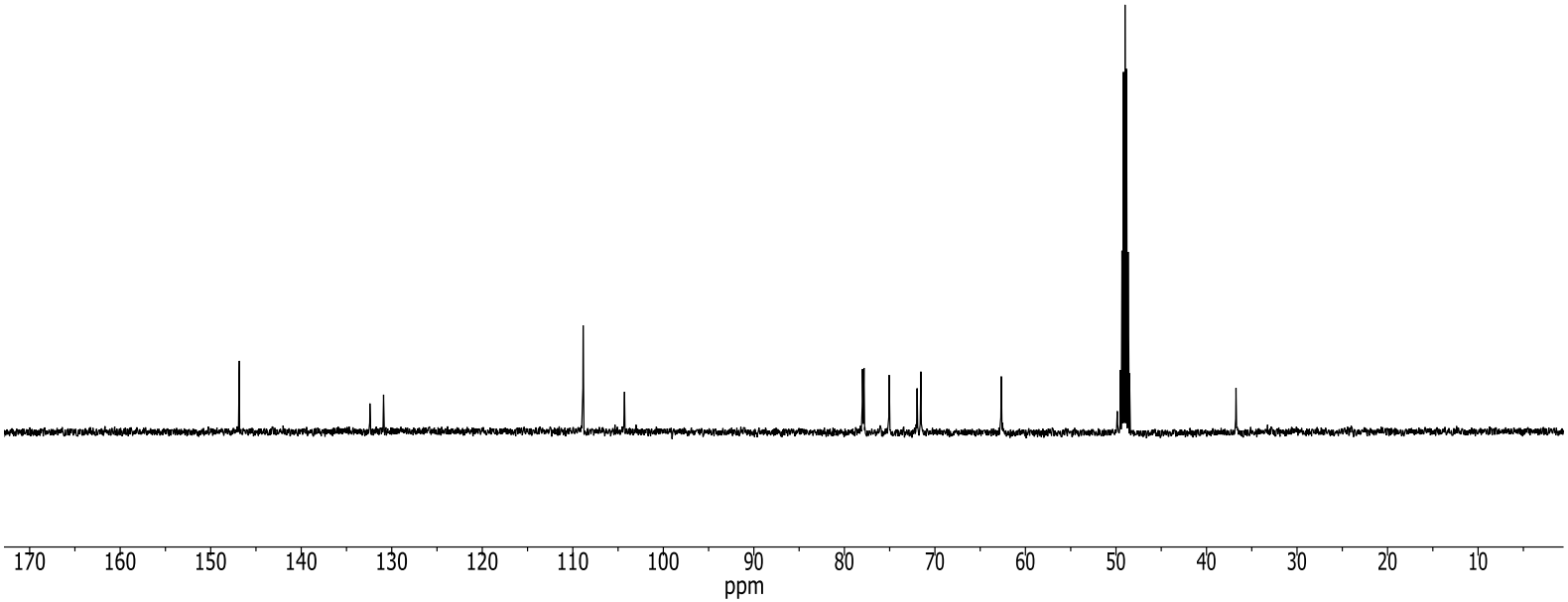

3,4,5-Tribenzyloxycinnamyl β-D-glucopyranoside (19)

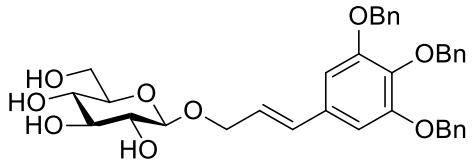

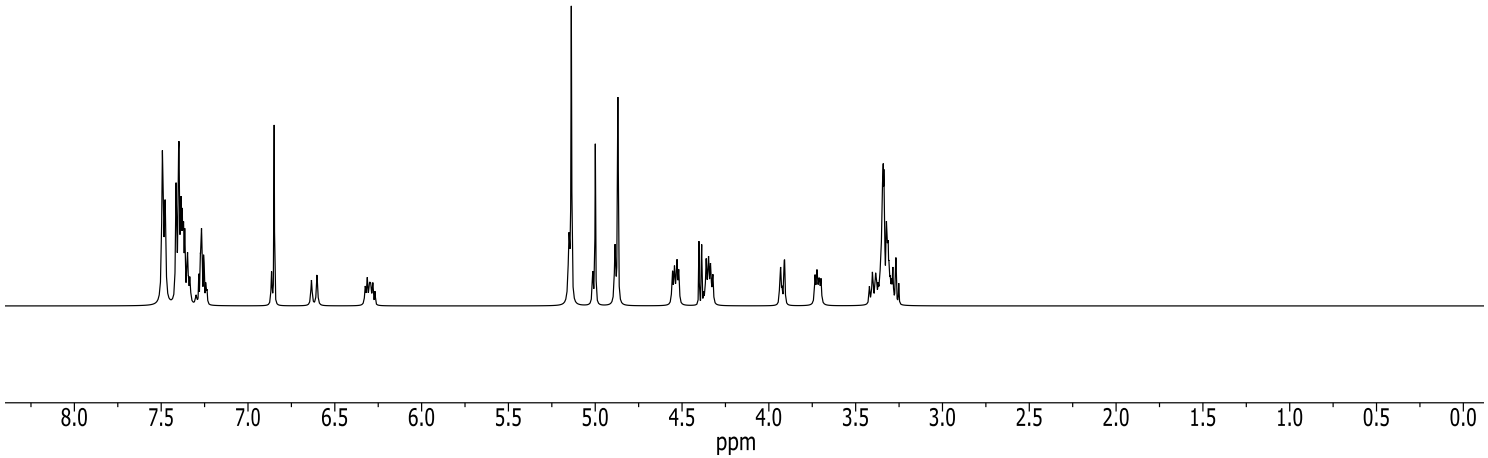

3,4,5-Tribenzyloxycinnamyl β-D-glucopyranoside (19)

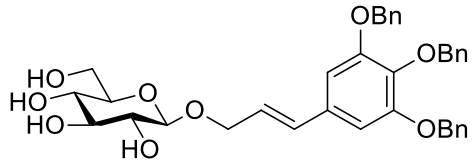

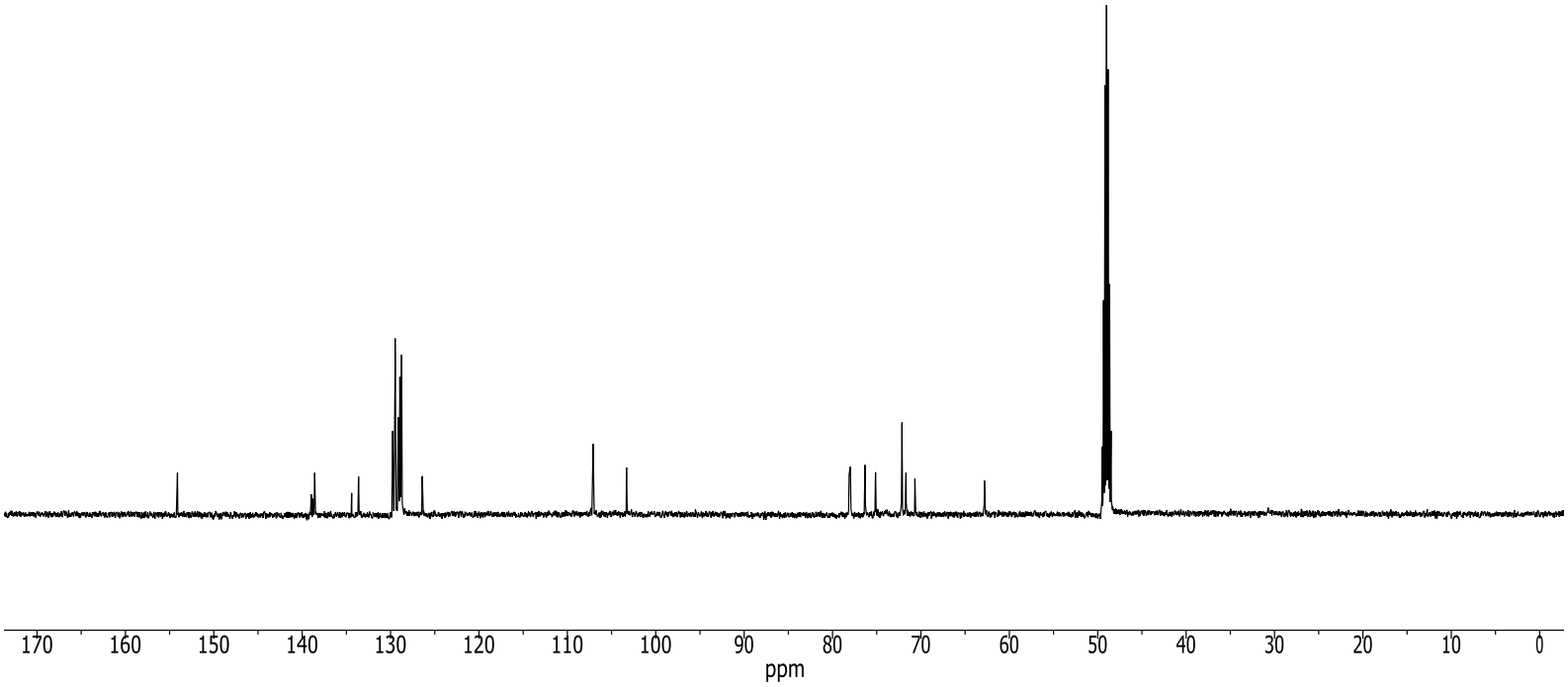

3-(3,4,5-Trihydroxyphenyl)propyl β-D-glucopyranoside (5)

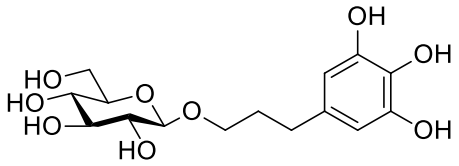

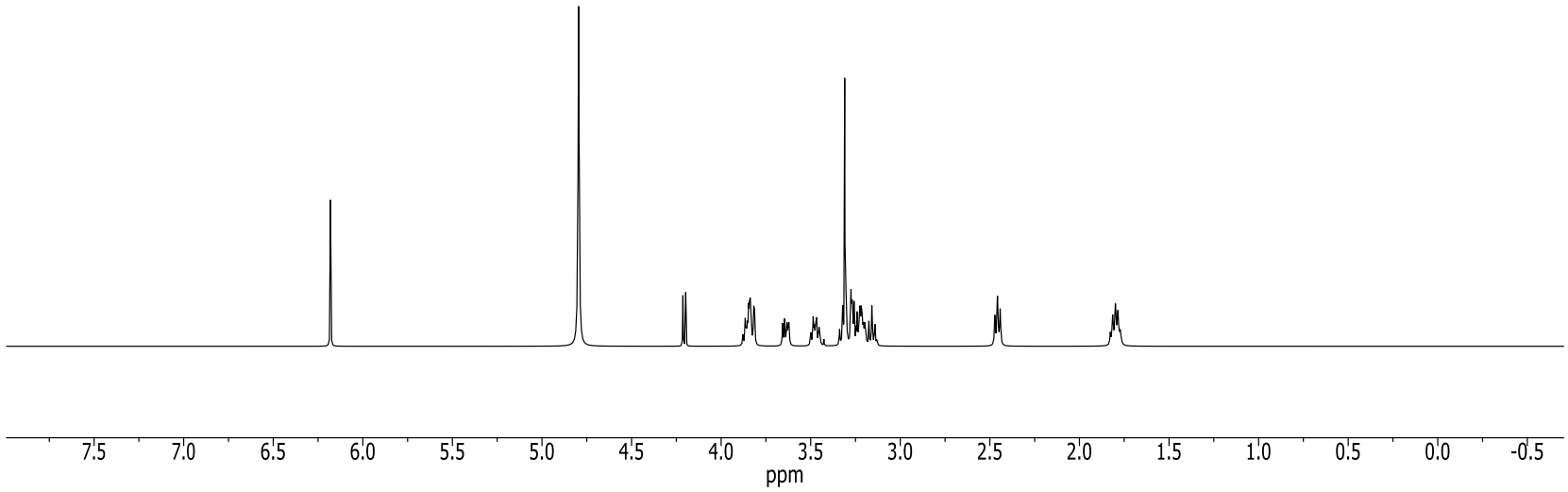

3-(3,4,5-Trihydroxyphenyl)propyl β-D-glucopyranoside (5)

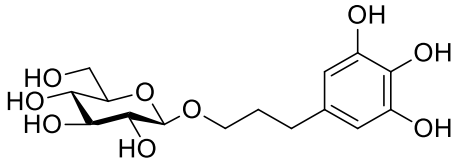

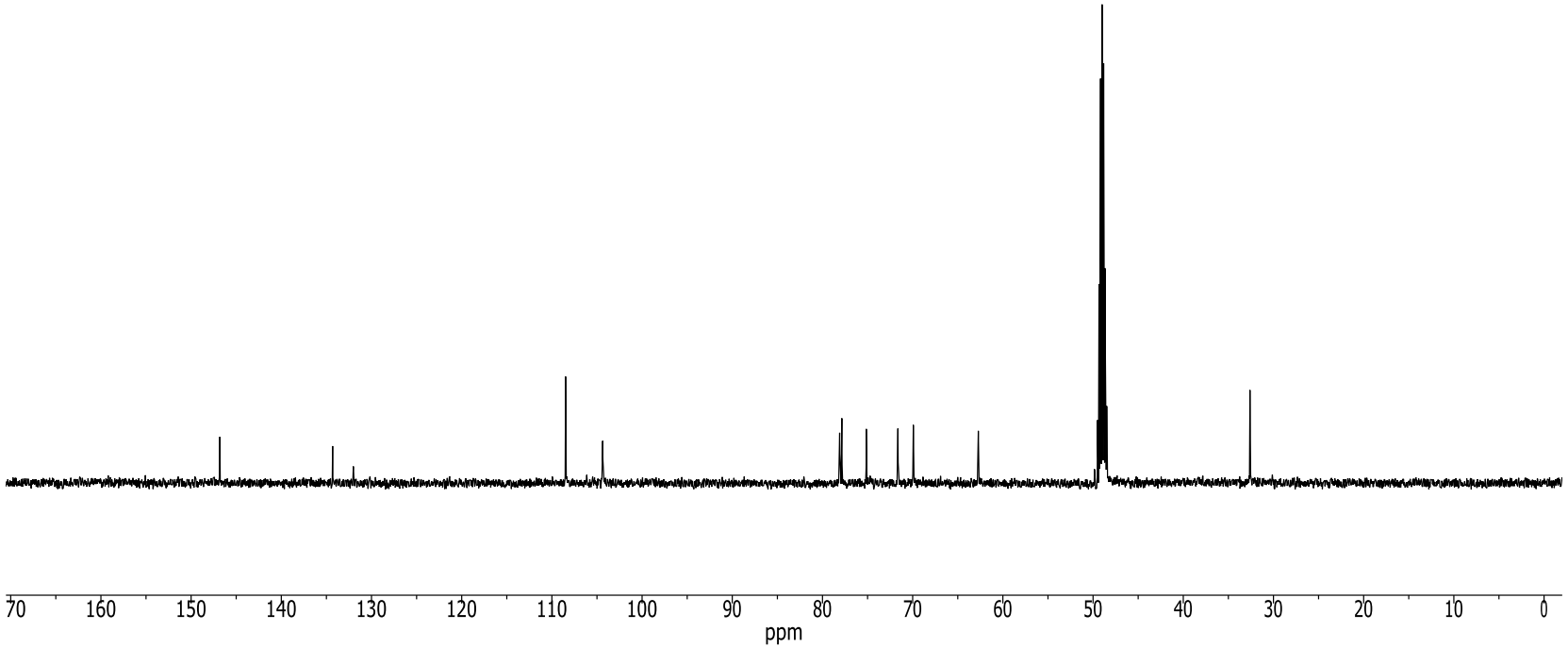

3,4,5-Tribenzyloxybenzyl azide (20)

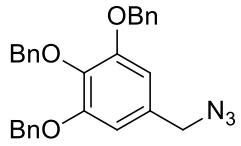

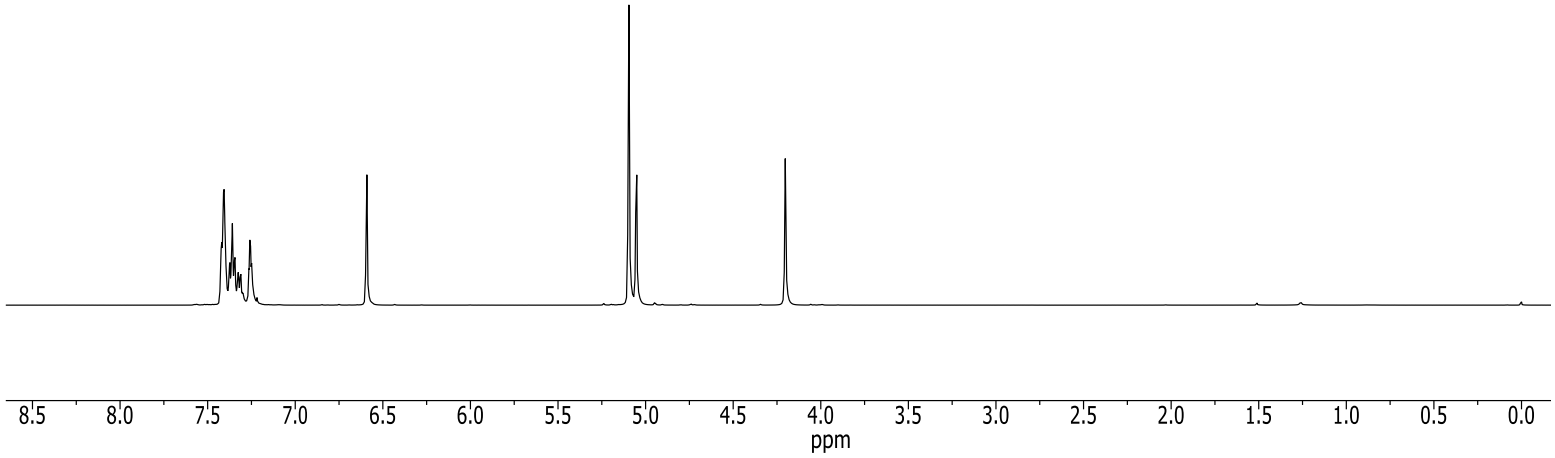

3,4,5-Tribenzyloxybenzyl azide (20)

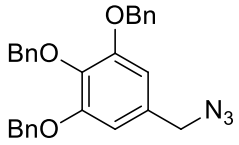

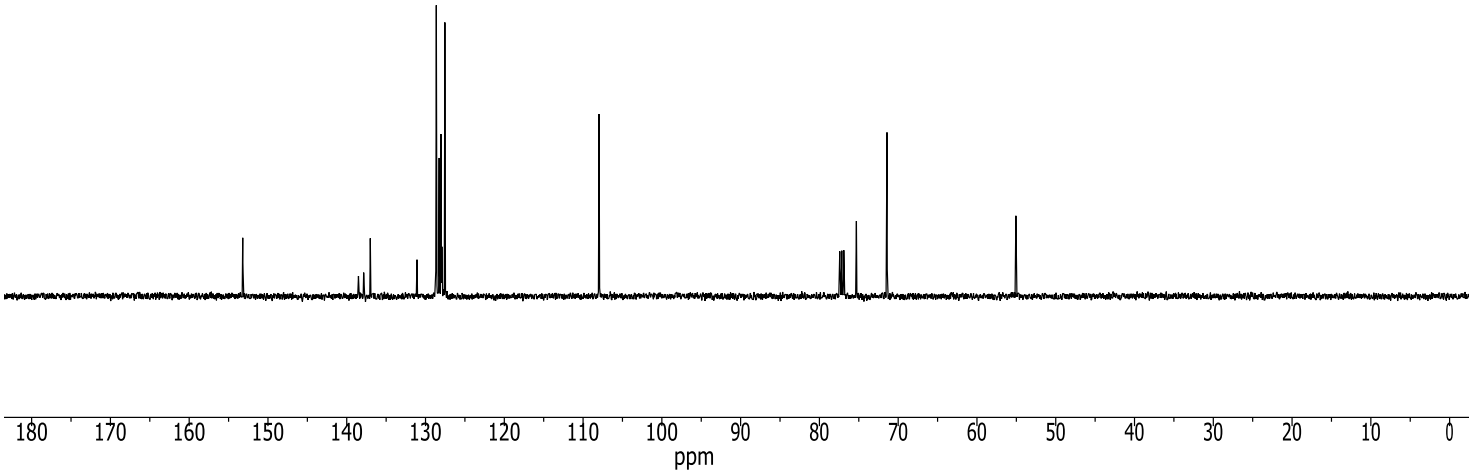

[1-(3,4,5-tribenzyloxybenzyl)-1,2,3-triazole-4-yl]methyl 2,3,4,6-tetra-*O*-acetyl β-D-glucopyranoside (22)

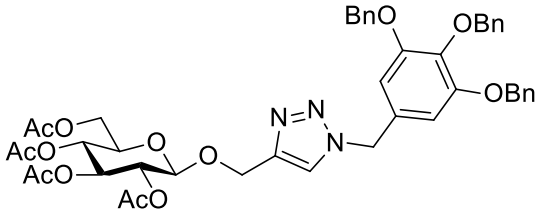

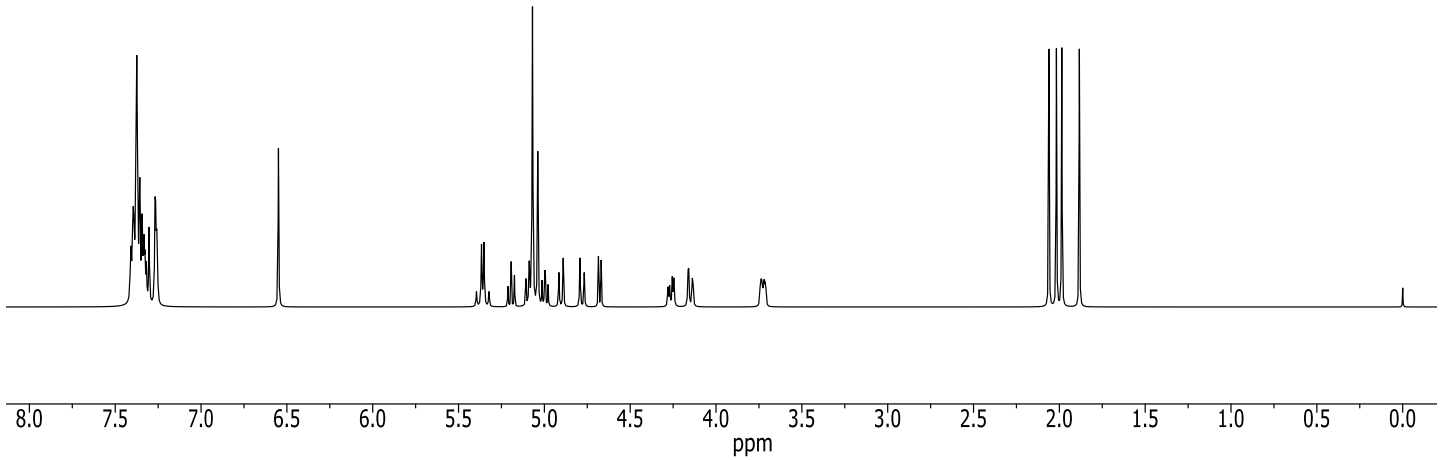

[1-(3,4,5-tribenzyloxybenzyl)-1,2,3-triazole-4-yl]methyl 2,3,4,6-tetra-*O*-acetyl β-D-glucopyranoside (22)

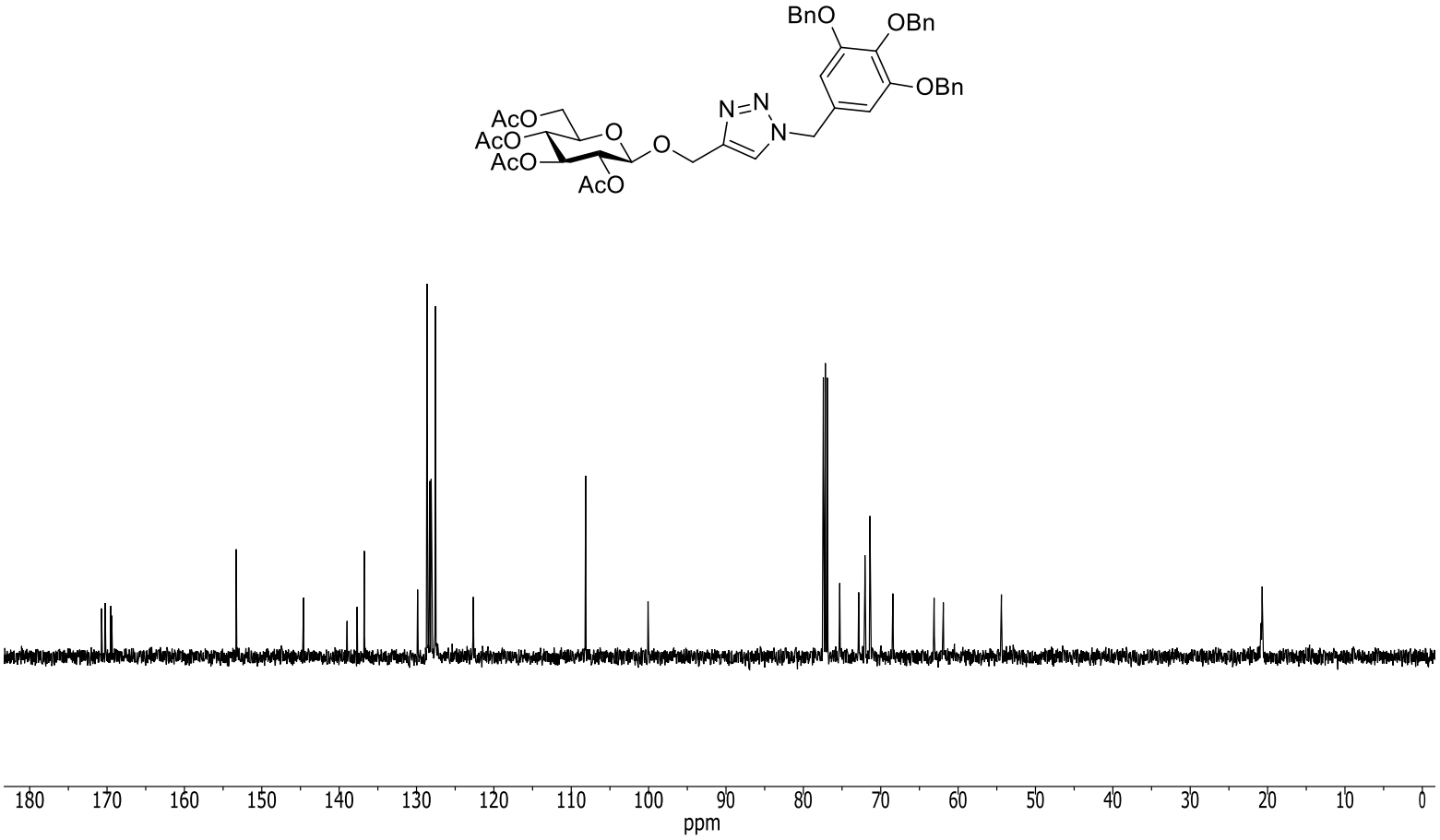

[1-(3,4,5-trihydroxybenzyl)-1,2,3-triazole-4-yl]methyl β-D-glucopyranoside (6)

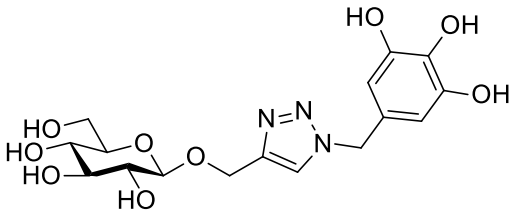

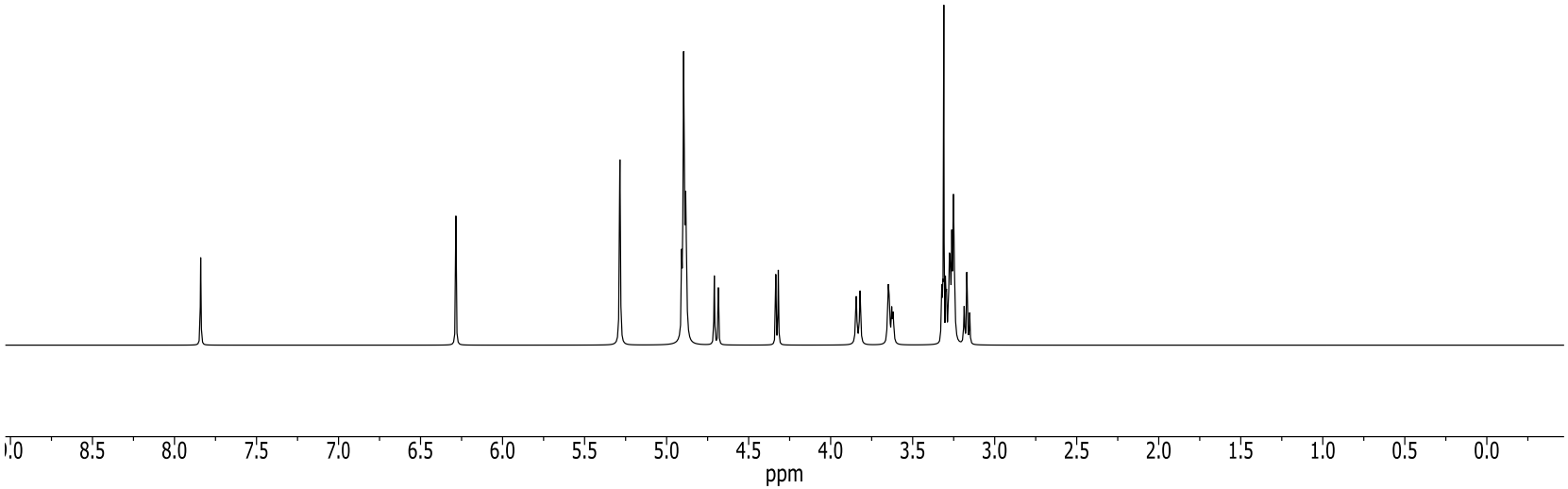

[1-(3,4,5-trihydroxybenzyl)-1,2,3-triazole-4-yl]methyl β-D-glucopyranoside (6)

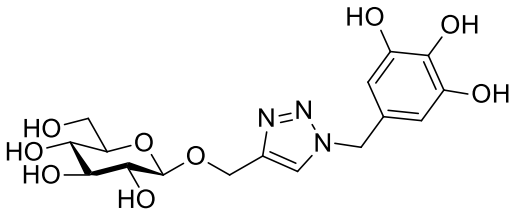

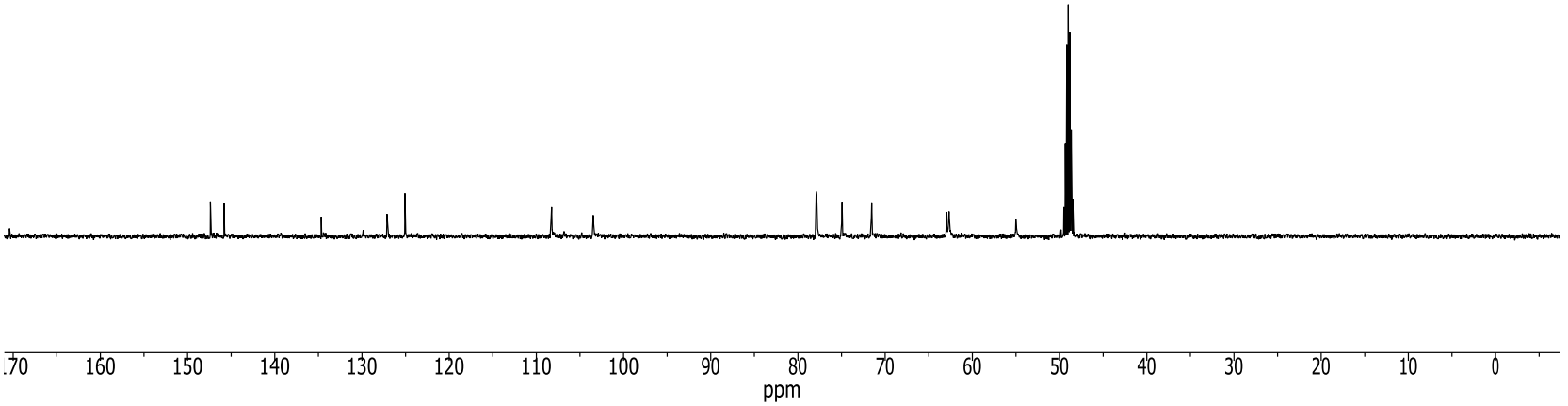

_N_-(3,4,5-Tri-_O_-benzylphenylacetyl)-2,3,4,6-tetra-_O_-acetyl β-D-glucopyranosylamine (24)

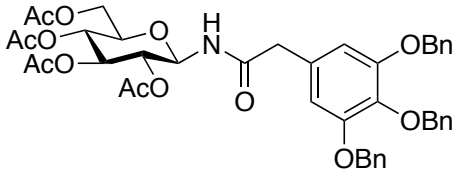

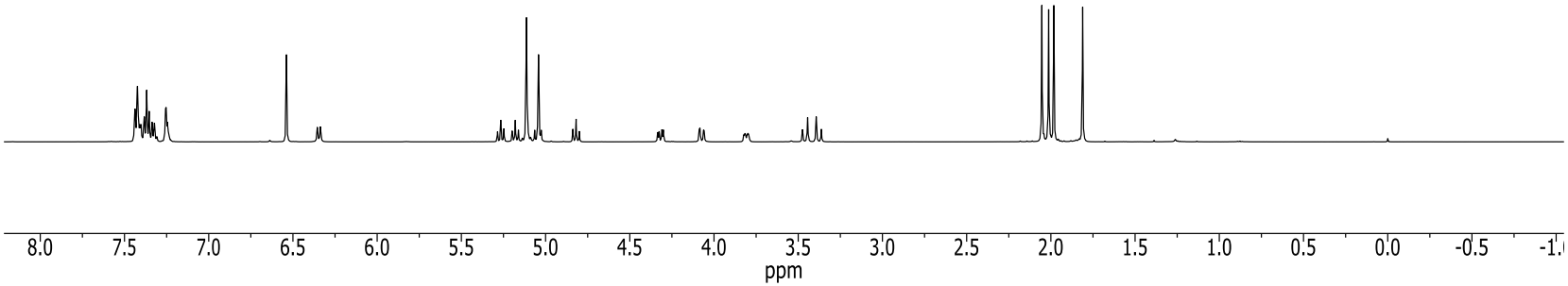

_N_-(3,4,5-Tri-_O_-benzylphenylacetyl)-2,3,4,6-tetra-_O_-acetyl β-D-glucopyranosylamine (24)

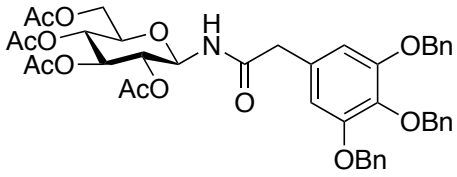

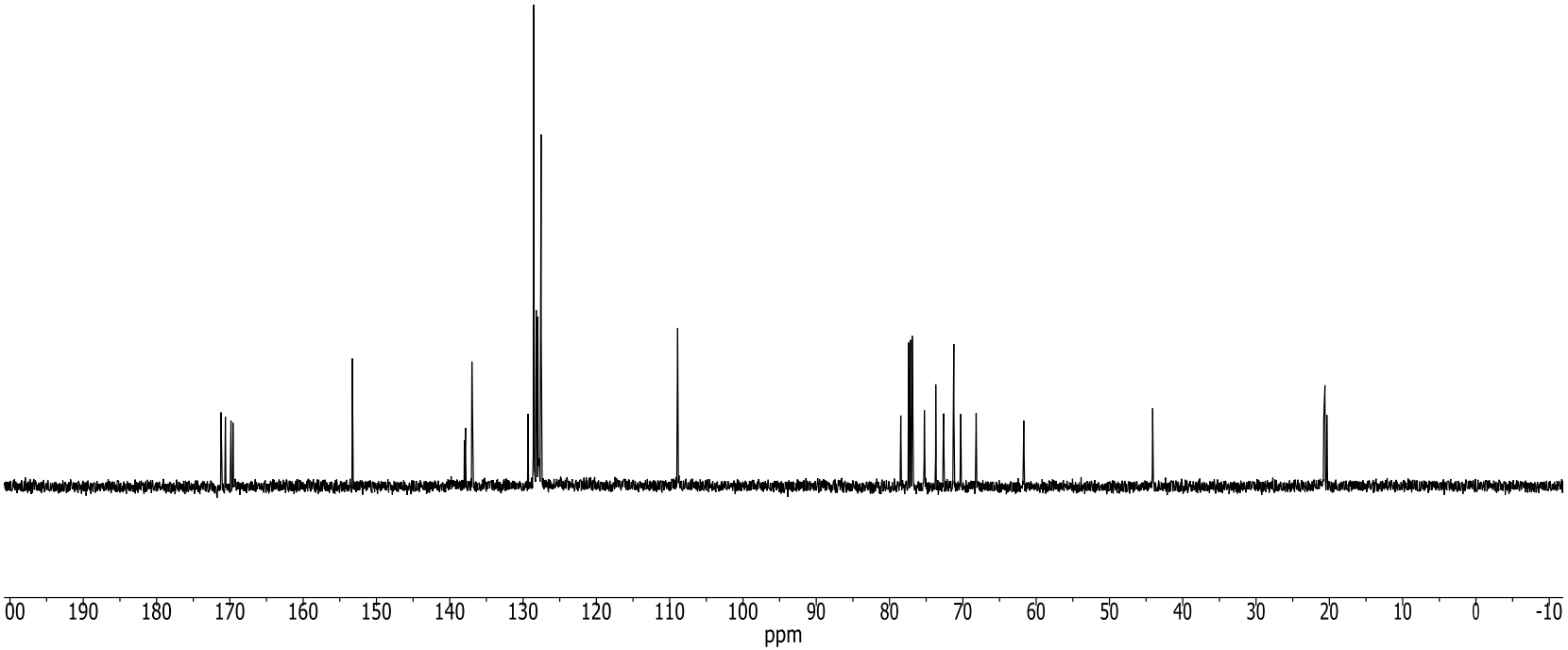

_N_-Phenylacetyl β-D-glucopyranosylamine (7)

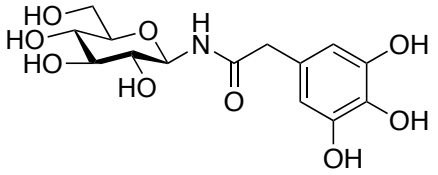

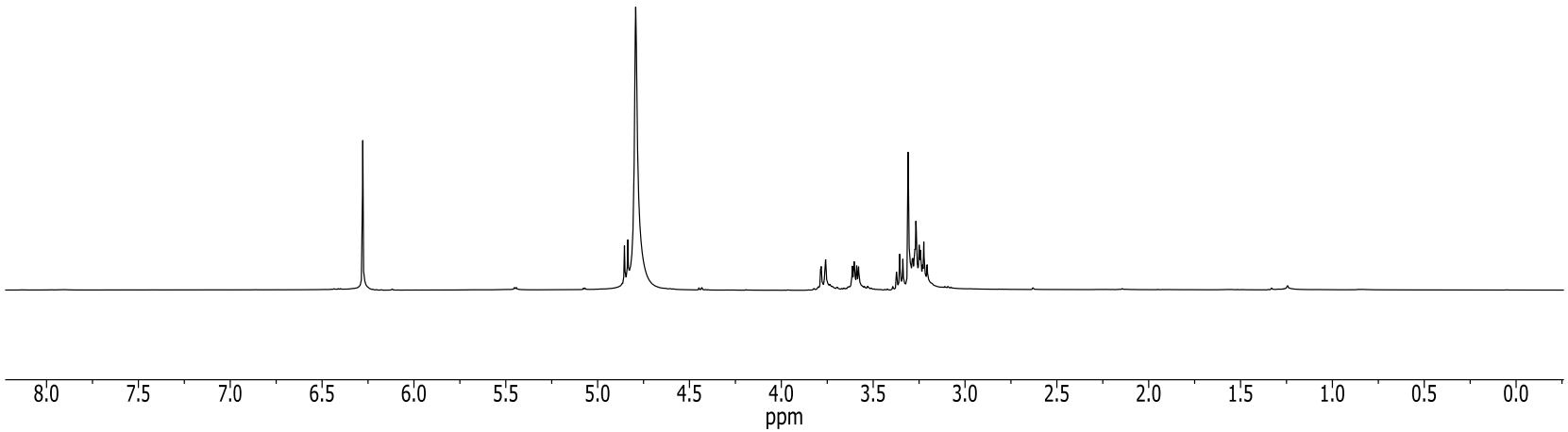

_N_-Phenylacetyl β-D-glucopyranosylamine (7)